

# Discovering “Semantics” in Super-Resolution Networks

Yihao Liu<sup>1 2\*</sup> Anran Liu<sup>1 4\*</sup> Jinjin Gu<sup>1 5</sup>  
Zhipeng Zhang<sup>2 6</sup> Wenhao Wu<sup>7</sup> Yu Qiao<sup>1 3</sup> Chao Dong<sup>1†</sup>  
<sup>1</sup>Shenzhen Institute of Advanced Technology, CAS  
<sup>2</sup>University of Chinese Academy of Sciences  
<sup>3</sup>Shanghai AI Lab <sup>4</sup>The University of Hongkong  
<sup>5</sup>University of Sydney <sup>6</sup>Institute of Automation, CAS <sup>7</sup>Baidu Inc.

## Abstract

*Super-resolution (SR) is a fundamental and representative task of low-level vision area. It is generally thought that the features extracted from the SR network have no specific semantic information, and the network simply learns complex non-linear mappings from input to output. Can we find any “semantics” in SR networks? In this paper, we give affirmative answers to this question. By analyzing the feature representations with dimensionality reduction and visualization, we successfully discover the deep semantic representations in SR networks, i.e., deep degradation representations (DDR), which relate to the image degradation types and degrees. We also reveal the differences in representation semantics between classification and SR networks. Through extensive experiments and analysis, we draw a series of observations and conclusions, which are of great significance for future work, such as interpreting the intrinsic mechanisms of low-level CNN networks and developing new evaluation approaches for blind SR.*

## 1. Introduction

The emergence of deep convolutional neural network (CNN) has given birth to a large number of new solutions to low-level vision tasks [7, 42, 41]. Among these progresses, image super-resolution (SR) has enjoyed a great performance leap. Compared with traditional methods (e.g., interpolation [15] and sparse coding[35, 36]), SR networks are able to produce more visually pleasing results with improved efficiency.

However, even if we have benefited a lot from the powerful CNNs, we have little knowledge about what happens in SR networks and what on earth distinguishes them from

traditional approaches. Does the performance gain merely come from more complex mapping functions? Or is there anything different inside SR networks, like classification networks with discriminative capability? On the other hand, as a classic regression task, SR is expected to perform a continuous mapping from LR to HR images. It is generally a local operation without the consideration of global context. But with the introduction of GAN-based models [19, 32], more delicate SR textures can be generated. It seems that the network has learned some kind of semantic, which is beyond our common perception for regression tasks.

Then, we may raise the question: are there any “semantics” in SR networks? If yes, do these semantics have different definitions from those in classification networks? Existing literatures cannot answer these questions, as there is little research on interpreting low-level vision deep models. Nevertheless, to discover the semantics in SR networks is of great importance. *It can not only help us further understand the underlying working mechanisms, but also guide us to design better networks and evaluation algorithms.*

In this study, we give affirmative answers to the above questions by unfolding the semantics hidden in super-resolution networks. Specifically, different from the artificially predefined semantics associated with object classes in high-level vision, semantics in SR networks are distinct in terms of **image degradations** instead of image contents. Thus, *the semantics in this paper have different indications for SR and classification networks.* More interestingly, such degradation-related semantics are spontaneously existing, without involving relevant data or pre-labelling. Our observation stems from a representative blind SR method – CinCGAN [37], and we further extend it to more common SR networks – SRResNet and SRGAN [19]. We have also revealed more interesting phenomena to help interpret the semantics, including the analogy to classification networks, the influential factors for semantic discovery, and the distinction of different degradations. We believe our findings could lay the groundwork for the interpretability of SR net-

\*The first two authors contributed equally (co-first authors). Email: liuyihao14@mails.ucas.ac.cn, liuar616@connect.hku.hk.

†Corresponding author. Email: chao.dong@siat.ac.cn.

works, and inspire better solutions for more challenging tasks, like blind SR for real-world images.

In summary, our contributions are mainly four-fold. 1) We have successfully discovered the “semantics” in SR networks, denoted as deep degradation representations (DDR). 2) We reveal the differences of semantics between classification and SR networks, for the first time. 3) We introduce a set of simple yet potential approach in analyzing and extracting the semantic information in SR networks. 4) Through extensive experiments and analysis, we draw a series of interesting observations and conclusions on DDR, which are of great significance for future work.

## 2. Related Work

**Super-resolution.** Super-resolution (SR) is a fundamental and representative task in low-level vision, which aims to reconstruct the high-resolution (HR) image from the corresponding low-resolution (LR) counterpart. SRCNN [7] is the first proposed CNN-based method for SR. Since then, a large number of deep-learning-based SR methods have been developed [8, 21, 43, 19, 42]. Generally, current CNN-based SR methods can be categorized into two groups. One is MSE-based method, which targets at minimizing the distortion (e.g., Mean Square Error) between the ground-truth HR image and super-resolved image to yield high PSNR values, such as SRCNN [7], FSRCNN [8], VDSR [16], EDSR [21], RCAN [43], SAN [5], etc. The other is GAN-based method, which incorporates generative adversarial network (GAN) and perceptual loss [14] to obtain realistic and perceptually pleasing results, such as SRGAN [19], ESRGAN [32], RankSRGAN [42], SROBB [26]. Recently, blind SR has attracted more and more attention [10, 2, 23, 31], since it targets at solving the most challenging scenarios with real-world degradation. A comprehensive survey for blind SR is newly proposed [22], which summarizes and compares the ideas and performance of existing methods. In this paper, we regard SR as a representative research object, and study its deep semantic representations, which can also draw inspirations on other low-level vision tasks.

**Network interpretability.** At present, most existing works on neural network interpretability focus on high-level vision tasks, especially for image classification. In a recent survey paper, Zhang *et al.* [44] systematically reviewed existing literatures on network interpretability and proposed a novel taxonomy to categorize them. Here we only discuss several classic works. By adopting deconvolutional networks [40], Zeiler *et al.* [39] projected the downsampled low-resolution feature activations back to the input pixel space, and then performed a sensitivity analysis to reveal which parts of the image are important for classification. Simonyan *et al.* [28] generated a saliency map from the gradients through a single backpropagation pass. Based on class

activation maps (CAM) [45], Selvaraju *et al.* [27] proposed Grad-CAM (Gradient-weighted CAM) to produce a coarse-grained attribution map of the important regions in the image, which was broadly applicable to any CNN-based architectures. For more information about the network interpretability literatures, please refer to the survey paper [44]. However, for low-level vision tasks, similar researches are rare. Most recently, a novel attribution approach called local attribution map (LAM) [9] was proposed to interpret super-resolution networks, which was used to localize the input features that influenced the network outputs. It inherited the previous gradient-guided attribution methods but was specially designed for SR networks. In our work, we interpret SR networks from another new perspective. We dive into their feature representations, and discover the deep semantics of SR networks. For more background knowledge, please refer to the supplementary file.

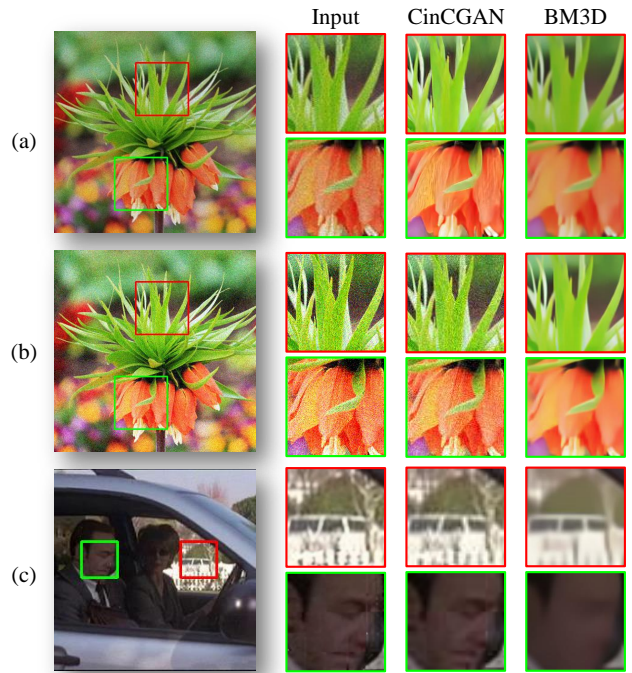


Figure 1. Different degraded input images and their corresponding outputs produced by CinCGAN [37] and BM3D [4]: (a) DIV2K-mild, (b) DIV2K-noise20 and (c) Hollywood. CinCGAN [37] is trained on DIV2K-mild dataset in an unpaired manner. If the input image conforms to the training data distribution, CinCGAN will generate better restoration results than BM3D, i.e., (a). Otherwise, it fails to deal with the input images (b)&(c). More specifically, it tends to ignore unseen noise/artifacts and keeps the input images untouched. On the other hand, the traditional method BM3D [4] has a stable performance and similar denoising effects on all input images, regardless of the input degradations. Please zoom in for best view.

### 3. Motivation

To discover semantics, we start with the scenario that could easily distinguish SR networks and traditional methods. It is well known that SR networks are superior to traditional methods in supervised learning, but are inferior in generalization ability. Thus we select the blind SR task, where the degradation models are unknown and the testing should be performed across different datasets. Traditional methods generally have a stable performance, and treat different images equally without distinction of degradation types. How about the SR networks, especially those designed for blind SR task?

CinCGAN [37] is a representative solution for real-world SR without paired training data. It maps a degraded LR to its clean version using data distribution learning before conducting SR operation. However, we find that, even if CinCGAN is developed for blind setting, it still has a limited application scope: if the degradation of the input image is not included in the training data, CinCGAN will fail to transfer the degraded input to a clean one. More interestingly, instead of producing extra artifacts in the image, it seems that CinCGAN does not process the input image and retain all the original defects. Readers can refer to Fig. 1 for an illustration, where CinCGAN performs well on testing image of DIV2K-mild dataset (same distribution as its training data), but produces unchanged results for other images with different degradation types. In other words, the network seems to figure out the specific degradation types within its training data distribution, and any distribution mismatch will make the network “turn off” its ability. For comparison, we further process the above three types of degraded images by a traditional denoising method BM3D [4]<sup>1</sup>. As shown in Fig. 1, for all input images with different degradation types, BM3D has a obvious and stable denosing performance. Although the results of BM3D may be mediocre (the image textures and details are largely over-smoothed), it does try to process every input image. This observation reveals that there is a significant discrepancy between traditional method and CNN-based method.

The above interesting phenomenon indicates that the network has learned more than a regression function, since it demonstrates the ability to distinguish among different degradation types. Inspired by this observation, we try to find any semantics hidden in CinCGAN, as well as in other SR networks.

<sup>1</sup>Note that BM3D is a denoising method while CinCGAN is able to upsample the resolution of the input image. Thus, after applying BM3D, we utilize bicubic interpolation to unify the resolution of the output image. This is reasonable as we only evaluate their denoising effects.

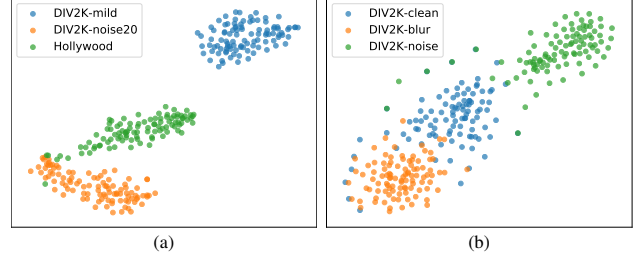


Figure 2. The projected deep feature representations are clustered by degradation types: (a) CinCGAN and (b) SRGAN-wGR.

### 4. Digging Out Semantics in Super-Resolution Networks

In this section, we first describe our analysis method. Then, we elaborate our findings on semantics in SR networks, as well as their differences from those in classification network.

#### 4.1. Analysis Method

As stated in Sec.3, CinCGAN treats LR inputs in different ways for different degradations. Since the final outputs are always derived from features in CNN layers, we start the exploration with feature maps, especially the deep ones potentially with more global and abstract information. To interpret the deep features of CNN, one common and rational way is to convert the high-dimensional CNN feature maps into lower-dimensional datapoints that can be visualized in a scatterplot. Afterwards, human can intuitively understand the data structures and the manifolds. Specifically, we adopt t-Distributed Stochastic Neighbor Embedding (t-SNE) [29], a popular algorithm in manifold learning, for dimensionality reduction. This technique can greatly capture the local structure of the high-dimensional data and simultaneously reveal global structure, such as the presence of clusters at several scales. Also, it has been successfully applied in previous works [6, 24, 34, 38, 30, 33, 13] for feature projection and visualization. In all the experiments, we first reduce the dimensionality of feature maps to a reasonable amount (50 in this paper) using PCA [12], then apply t-SNE to project the 50-dimensional representation to two-dimensional space, after which the results are visualized in a scatterplot. Moreover, we also introduce several indicators to better illustrate and quantitatively evaluate the distributions of visualized datapoints. More details about the t-SNE and the introduced quantitative indicators are depicted in the supplementary file.

#### 4.2. How do the Semantics in Super-Resolution Networks Look Like?

Equipped with the t-SNE technique, we extract features from the deep layers of CinCGAN for visualization. Specifically, as discussed in Sec.3, since CinCGAN performs dif-

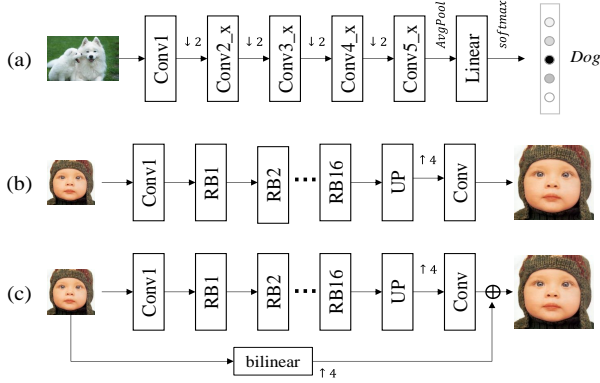


Figure 3. Simplified diagrams of different architectures. (a) ResNet18 [11] for classification. “Conv2\_x” represents the 2nd group of residual blocks. (b) SRResNet-woGR. Plain SRResNet [19] without image global residual. “RB1” represents the 1st residual block. (c) SRResNet-wGR, which learns the residual image.

ferently on various input datasets, we further compare the features generated from three different testing datasets: 1) DIV2K-mild: the original training and testing data in CinCGAN, which is synthesized from DIV2K [1] dataset. It contains noise, blur, pixel shifting and other degradations. 2) DIV2K-noise20: add Gaussian noises with noise level  $\sigma = 20$  to the DIV2K set, making it perceptually similar to DIV2K-mild. 3) Hollywood100: 100 images selected from Hollywood dataset [18], containing real-world old film frames with unknown degradation. Each testing dataset includes 100 images.

The visualization results are shown in Fig.2(a). One can see that there exists a discriminative clustering for datapoints from the same dataset. While for different datasets, even if their image contents are the same, their corresponding datapoints still belong to different clusters.<sup>2</sup> This observation conforms to our observation that CinCGAN *does* treat inputs with various degradations in different ways. More importantly, it naturally reveals the semantics contained in CinCGAN, which are closely related to the degradation types rather than image content.

**From CinCGAN to Generic SRGAN.** Based on the above findings, we are curious about whether this kind of degradation-related semantics is universal among SR networks, especially for supervised SR methods. Therefore, referring to [19, 32], we design a generic GAN-based SR architectures SRGAN-wGR<sup>3</sup> to repeat the visualization experiment. Note that, we here adopt *image global residual learning* scheme where the generator is designed to learn

<sup>2</sup>Note that the class labels in the scatterplots are only used to assign a color/symbol to the datapoints for better visualization. The class information is not used by t-SNE to determine the spatial coordinates of the data after dimension reduction.

<sup>3</sup>SRGAN [19] is a renowned GAN-based SR model, in which the generator consists of several stacked residual blocks. Following ESRGAN [32], we remove all the BN layers in the generator for better performance.

the image residual rather than to directly learn the output. In Sec. 5.1, we reveal that the global residual (GR) has an important impact on the learned features, especially for MSE-based SR networks. In this paper, we use “wGR” and “woGR” to denote whether the network has a global residual or not. Fig. 3 briefly illustrates different architectures.

SRGAN-wGR is trained using the widely-adopted DIV2K dataset [1] with *only* bicubic-downsampled LR inputs. According to the common degradation modelling in low-level vision, we use three datasets with different degradation types for testing: 1) DIV2K-clean: the original DIV2K validation set containing only bicubic down-sampling degradation, which conforms to the training data distribution. 2) DIV2K-blur: apply Gaussian blur kernel on the DIV2K-clean set, thus making it contain extra blurring degradation. The kernel width is randomly sampled from [2, 4] for each image and the kernel size is fixed to  $15 \times 15$ . 3) DIV2K-noise: add Gaussian noises to the DIV2K-clean set. The noise level is randomly sampled from [5, 30] for each image. Hence, these three testing datasets are aligned in image content but different in degradation types.

Visualization result for SRGAN is given in Fig.2(b), where a clustering trend similar to CinCGAN is clearly demonstrated. This evidence for existence of degradation-related semantics is even much stronger, since the three testing sets now share exactly the same contents but still have distinct discrepancy in clustering.

There, we successfully find the semantics hidden in SR networks. They are perceivable to human when visualized in low-dimensional space. Specifically, *semantics in SR networks are in terms of degradation types regardless of the image contents*. Simply but vividly, we name this kind of semantics as deep degradation representations (DDR).

**Summary and Discussion.** Through above experiments and analysis, we have answered the question that “can we find semantics in super-resolution networks?” as well as “what are the semantics in SR networks?”, by introducing the deep degradation representations (DDR). One may argue that images with different degradation types are spontaneously different, which naturally leads to different feature representations extracted by the networks. However, different networks tend to extract features containing different semantic information. For example, in Sec. 4.3, we show that classification networks are prone to learn abstract representations that are related with the image content (object category). Instead, the feature representations of SR networks demonstrate discriminability on image degradation types other than image content. This is non-trivial for low-level vision tasks such as super-resolution networks, due to the lack of predefined semantic labels during training, but we succeed in finding the “semantics” in SR networks. **During training, the SR networks are only provided with down-sampled clean data, without any exposure to blur/noise**



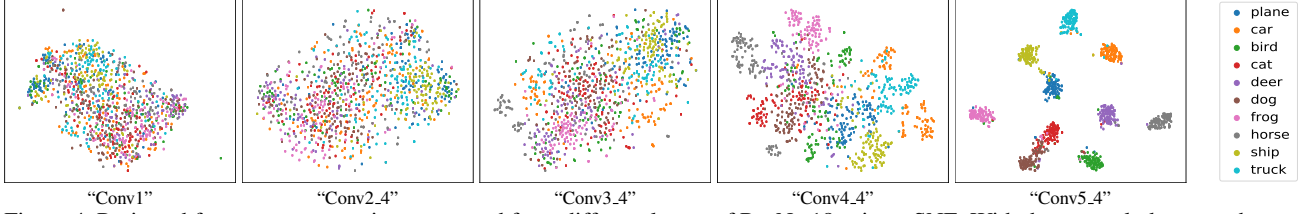


Figure 4. Projected feature representations extracted from different layers of ResNet18 using t-SNE. With the network deepens, the representations become more discriminative to object categories, which clearly shows the semantics of the representations in classification.

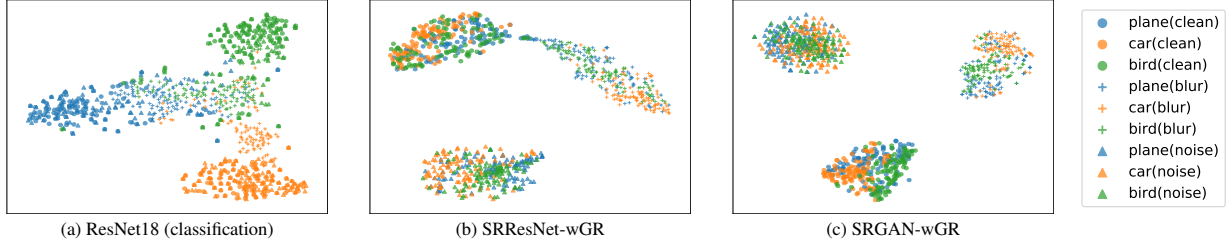


Figure 5. Feature representation differences between classification and super-resolution networks. The same object category is represented by the same color, and the same image degradation type is depicted by the same marker shape. For the classification network, the feature representations are clustered by the same color, while the representations of SR network are clustered by the same marker shape, suggesting there is a significant difference in feature representations between classification and super-resolution networks. Better viewed on the screen.

**data. Nevertheless, when testing, the SR networks can produce deep representations that can distinguish different degradation types. This phenomenon is never discussed before.** Moreover, in Sec. 5.1, we show that not all SR network structures can easily obtain DDR, suggesting that this phenomenon is *not* simply caused by different inputs. Further, in the next section, we directly reveal the differences between classification and SR networks in semantic representations.

### 4.3. Differences in Semantics between Classification and Super-Resolution Networks

In this section, we directly compare the differences in representation semantics between classification and SR networks, aiming to reveal the uniqueness of degradation-related semantics for SR networks.

Classification is the most representative task in high-level vision, where artificially predefined semantic labels on object classes are given for target images. Due to the clearly defined semantics, classification networks are naturally endowed with semantic discrimination. Without loss of generality, we choose ResNet18 [11] as the classification backbone and conduct experiments on CIFAR10 dataset [17]. More results on various backbones are in the supplementary file. We extract the forward feature maps of each input testing image<sup>4</sup> at different network layers. Fig. 3(a) concisely describes the architecture of ResNet18.

From the visualization results in Fig. 4, it can be observed that as the network deepens, the extracted feature

representations produce obvious clusters, i.e., the learned features are increasingly becoming semantically discriminative. Further, such discriminative *semantics in classification networks are coherent with the artificially predefined labels* (semantic categories). This is an intuitive and natural observation, on which lots of representation and discriminative learning methods are based [34, 25, 20, 33].

Now, we compare the differences between classification and super-resolution networks in representation semantics. Specifically, we add blur and noise degradation to the CIFAR10 testing images, and then investigate the feature representations of classification and SR networks.

As shown in Fig. 5, after adding blur or noise to the data, the deep representations obtained by classification network (ResNet18) are still clustered by object categories, which indicates that the features extracted by the classification network focus more on high-level object class information, rather than low-level image degradation information. On the contrary, the deep representations obtained by SR networks (SRResNet-wGR and SRGAN-wGR) are clustered with regard to degradation types. In other words, features of the same object category are not clustered together, while those of the same degradation type are clustered together, showing different “semantic” discriminability from classification network. This phenomenon intuitively illustrates the differences in the deep semantic representations between SR and classification networks, i.e., degradation-related semantics and content-related semantics. Fig. 6 concisely illustrates the differences in semantics between classification and SR networks.

<sup>4</sup>For efficiency and convenience, we selected 1000 testing images in total (100 of each category).

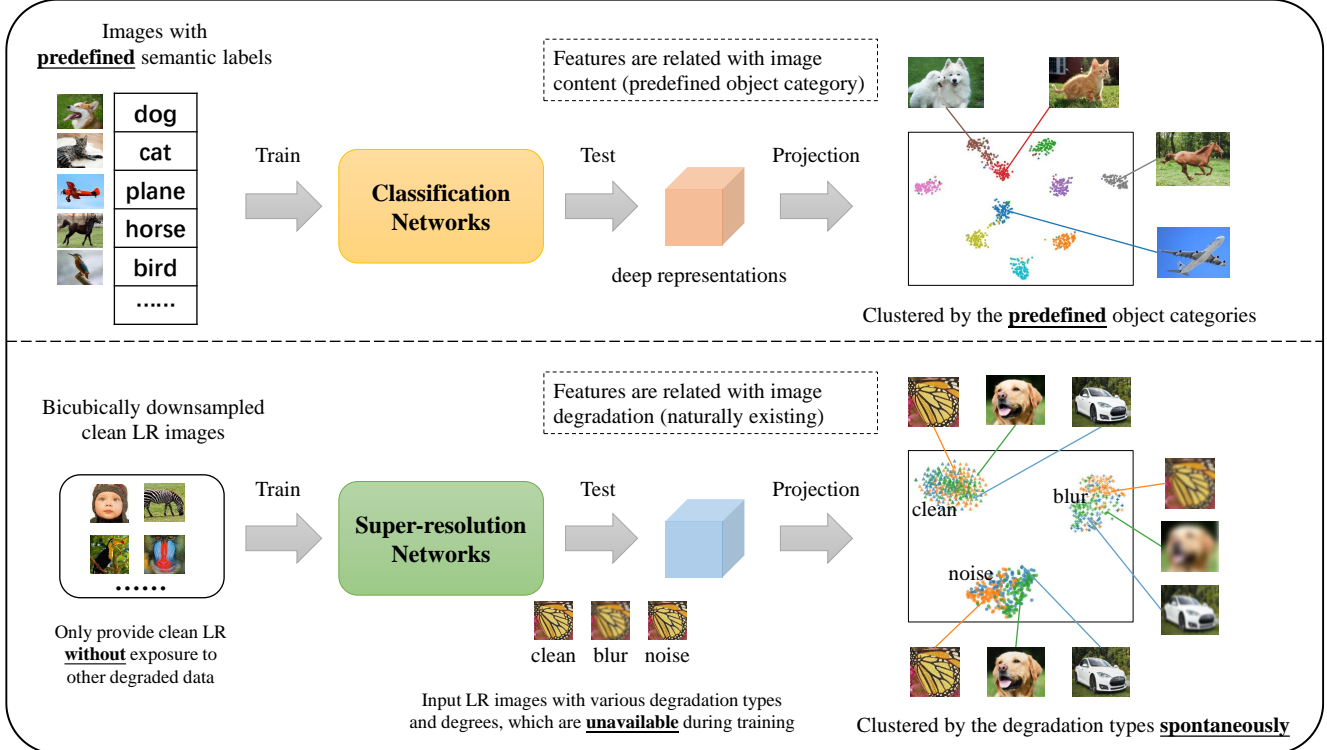


Figure 6. For classification networks, the semantics of deep feature representations are coherent with the artificially predefined labels (object categories). When training, each image is assigned with a specific object label as supervision signal. Thus, the networks learn to extract features that are discriminative for the object categories. Such semantic representations are artificially predefined and are dependent on the given training dataset. However, for super-resolution networks, the learned deep representations have different kind of “semantics” from classification. During training, the SR networks are only provided with bicubically downsampled LR images (without blur or noise), i.e., there is not any supervision signal related to image degradation information and there is no any data exposure to degraded images. Nevertheless, if we feed the trained SR networks with images with various degradations, the deep representations are spontaneously discriminative to different degradations. It is interesting that the SR networks can learn to extract features that are correlated with image degradation information, without any predefined labels or degradation priors. Notably, not arbitrary SR network has such property. In Sec. 5.1, we find two factors that can facilitate the SR network to extract such degradation-related representations, i.e., adversarial learning (GAN) and global residual learning (GR).

## 5. Further Investigation of Deep Degradation Representations

In the previous sections, we have established the notion of deep degradation representations (DDR) and drawn the significant observation on their differences from semantics in classification network. In this section, we further investigate the characteristics of DDR, and make some preliminary interpretations on the formation of DDR.

Moreover, we introduce Calinski-Harabaz Index (CHI) [3] to quantitatively evaluate the semantic discriminability, which can provide some rough yet practicable measures for reference. The CHI score is higher when clusters are well separated, which indicates stronger semantic discriminability. More details about the quantitative indicators are described in the supplementary file.

### 5.1. Two Factors for Discriminability of DDR

Although degradation-related semantics, i.e. DDR, have been dug out in SR networks, including CinCGAN, SRGAN-wGR and SRResNet-wGR, we further discovered in experiments that this semantic is not naturally discriminative for an arbitrary SR network structure. In this section, we introduce two crucial factors that can help effectively extract the above “semantic” information, i.e., image global residual learning (GR), and generative adversarial training (GAN-based). Based on GR, we demonstrate that there is a distinct discrepancy between MSE-based and GAN-based SR methods in feature representations: MSE-based methods have to exploit GR so as to obtain degradation-related semantics. Otherwise, the features are not discriminative for degradation information, especially for the blur degradation. GAN-based methods can obtain such semantics more easily, no matter whether there is GR or not (though GR can

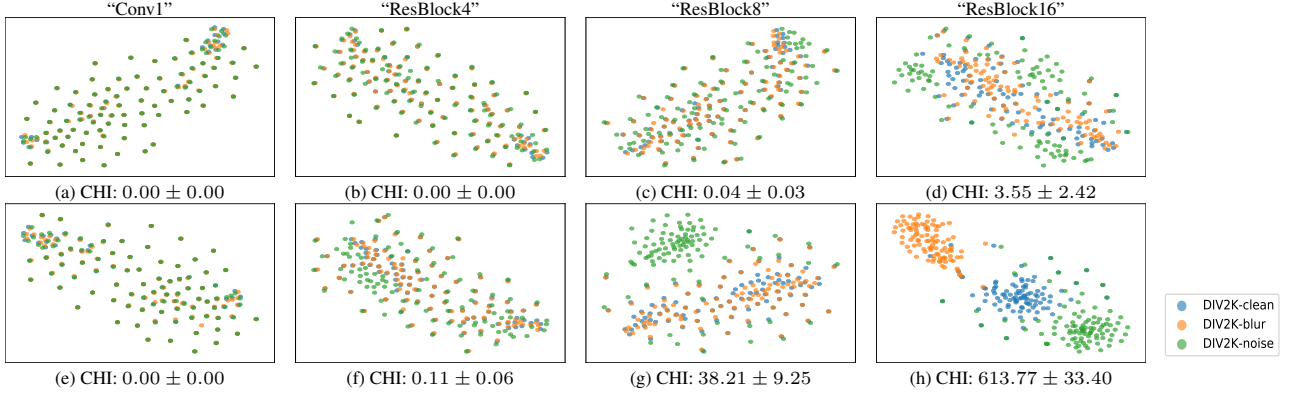


Figure 7. Projected feature representations extracted from different layers of SRResNet-woGR (1st row) and SRResNet-wGR (2nd row) using t-SNE. With image global residual (GR), the representations of MSE-based SR networks show discriminability to degradation types.

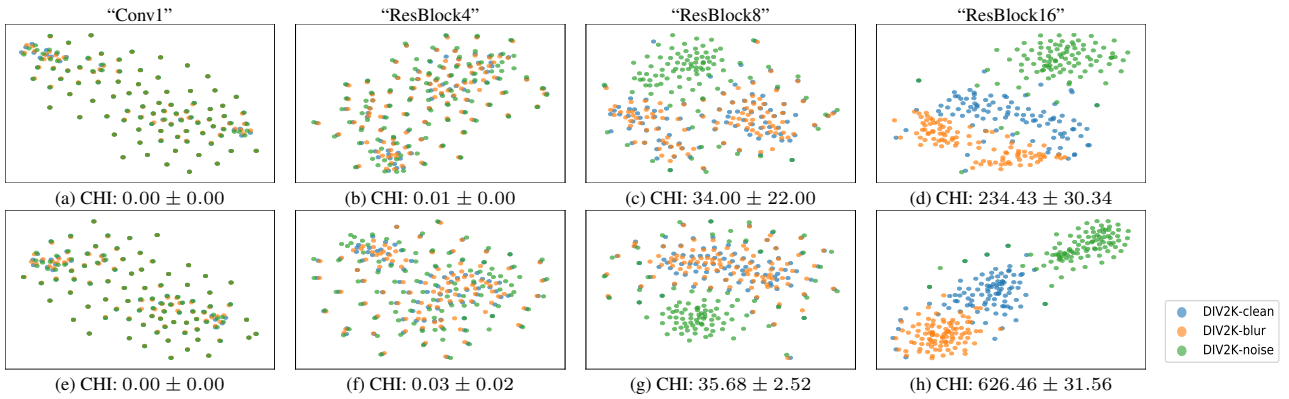


Figure 8. Projected feature representations extracted from different layers of SRGAN-woGR (1st row) and SRGAN-wGR (2nd row) using t-SNE. Even without GR, GAN-based SR networks can still obtain deep degradation representations.

further enhance the discriminability).

**Global Residual Learning vs. Plain Learning.** We train two SRResNet-like networks, one of which has a global residual (GR) path and the other does not, as shown in Fig. 3. Specifically, SRResNet-wGR learns the image residual through deep networks and adds it to the bilinearly upsampled input, while SRResNet-woGR directly learns to predict the final result from the input. Again, DIV2K [1] dataset is used for training, where the LR inputs are down-sampled by bicubic interpolation from HR images as in most literatures. Readers can refer to the supplementary file for more details.

Similar to the analysis techniques in Sec. 4, after testing on three datasets, we first obtain the deep features extracted from different layers of the networks and then use t-SNE for visualization analysis. Results are shown in Fig. 7.

From the experimental results, we can draw the following important observations: 1) For MSE-based SR method, global residual learning (GR) is essential for producing discriminative feature representations on degradation types. To be specific, the features in “ResBlock16” of SRResNet-wGR have shown distinct discriminability, where the clean, blur, noise data are clustered separately. On the contrary,

SRResNet-woGR shows no discriminability on such degradations even in deep layers. This phenomenon reveals that global residual has a paramount impact on the learned feature representations. It is inferred that learning the global residual could remove most of the content information of input image and make the network concentrate more on the contained degradation, thus the learned representations are discriminative. In Sec. 5.3, this claim is also corroborated by visualizing the feature maps: with GR, the learned feature maps tend to contain less information of image content (e.g., shape and structure). 2) As the network deepens, feature representations of SRResNet-wGR become more separable and discriminative. Note that this is similar to the discriminability of the feature representations in the classification network (Sec.4.3), except that the representations here are discriminative to the degradation types. Note that VDSR [16] first introduces GR into SR, but with a different purpose as our paper. In VDSR, GR is mainly proposed for fast convergence and better SR results. It does all testing on clean data. We discover/interpret the function of GR from another perspective: when receiving different degraded inputs, GR can help the network extract more degradation-related features without prior data/labels that are involved

with degradation information.

**MSE-based Method vs. GAN-based Method.** MSE-based and GAN-based method are currently two prevailing trends in CNN-based SR methods, among which the representatives are SRResNet and SRGAN. The optimization objective and loss functions of MSE-based and GAN-based SR methods are introduced in detail in the supplementary file. Previous studies only reveal that the visual effects of MSE-based and GAN-based methods are different, but the differences between their feature representations were rarely discussed. Since their learning mechanisms are quite different, will there be discrepancy in their deep feature representations? We will try to answer this question in the following.

For fair comparison, we adopt the same architectures as SRResNet-wGR and SRResNet-woGR to serve as the generators, and construct the discriminator adopted in SRGAN [19]. Consequently, we build two corresponding GAN-based models, namely SRGAN-wGR and SRGAN-woGR. After training, we perform the same test and analysis process mentioned earlier. The results are depicted in Fig. 8.

From the results, we obtain the following observations: 1) For GAN-based method, whether there is global residual (GR) or not, the deep features are bound to be discriminative to degradation types. As shown in Fig. 8(d), the deep representations in “ResBlock16” of SRGAN-woGR have already been clustered according to different degradation types. This clearly suggests that the learned deep representations of MSE-based method and GAN-based method are dissimilar. GAN-based method can obtain deep degradation representations without global residual. This also implies that adversarial learning can help the network learn more informative features for low-level degradations instead of image content. 2) Global residual can further enhance the representation discriminability to degradation types, as compared in Fig. 8(d) and Fig. 8(h). The quantitative evaluations are also in accordance with the visualization results. More quantitative analyses are included in the supplementary file.

## 5.2. Exploration on Different Degradation Degrees

In previous sections, we introduce deep degradation representations by showing that the deep representations of SR networks are discriminative to different degradation types (e.g., clean, blur and noise). How about the same degradation type but with different degraded degrees? Will the deep representations still be discriminative to them? To explore this question, more experiments and analysis are performed.

We test super-resolution networks on degraded images with different noise degrees and blur degrees. The results are depicted in Table. 1 and Fig. 9. It can be seen that the deep degradation representations are discriminative not only to cross-degradation (different degradation types) but

also to intra-degradation (same degradation type but with different degrees). This suggests that even for the same type of degradation, different degradation degrees will also cause significant differences in features. The greater the difference between degradation degrees, the stronger the discriminability of feature representations. This also reflects another difference between the representation semantics of super-resolution network and classification network. For classification, the semantic discriminability of feature representations is generally discrete, because the semantics are associated with discrete object categories. Nevertheless, there appears to be a spectrum (continuous transition) for the discriminability of the deep degradation representations, i.e., the discriminability has a monotonic relationship with the divergence between degradation types and degrees. For example, the degradation difference between noise levels 10 and 20 is not that much distinct, and the discriminability of feature representations is relatively smaller, comparing with noise levels 10 and 30.

From Table 1, there are notable observations. 1) Comparing with blur degradation, noise degradation is easier to be discriminated. Yet, it is difficult to obtain deep representations that have strong discriminability for different blur levels. Even for GAN-based method, global residual (GR) is indispensable to obtain representations that can be discriminative to different blur levels. 2) The representations obtained by GAN-based method have more discriminative semantics to degradation types and degrees than those of MSE-based method. 3) Again, global residual can strengthen the representation discriminability for degradations.

## 5.3. Visualization of Feature Maps

So far, we have successfully revealed the degradation-related semantics in SR networks with dimensionality reduction. In this section, we directly visualize the deep feature maps extracted from SR networks to provide some intuitive and qualitative interpretations. Specifically, we extract the feature maps obtained from four models (SRResNet-wGR, SRResNet-woGR, SRGAN-wGR and SRGAN-woGR) on images with different degradations (clean, blur4, noise20), respectively. Then we treat each feature map as a one channel image and plot it. The visualized feature maps are shown in Fig. 10. We select 8 feature maps with the largest eigenvalues for display. The complete results are shown in the supplementary file.

**Influence of degradations on feature maps.** From Fig. 10(a), we can observe that the deep features obtained by SRResNet-woGR portray various characteristics of the input image, including edges, textures and contents. In particular, we highlight in “red rectangles” the features that retain most of the image content. As shown in Fig. 10(b), after applying blur and noise degradations to the input image, the



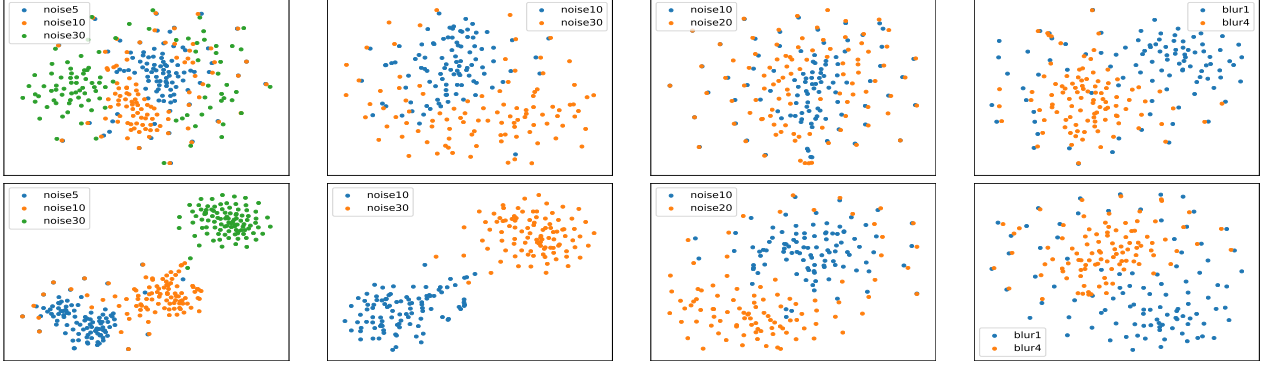


Figure 9. Even for the same type of degradation, different degradation degrees will also cause differences in features. The greater the difference between degradation degrees, the stronger the discriminability. **First row:** SRResNet-wGR. **Second row:** SRGAN-wGR.

		Cross-degradation	Intra-degradation (degradation degrees)			
	structure	Clean-Blur-Noise	Noise{5,10,30}	Noise{10,30}	Noise{10,20}	Blur{1,4}
SRResNet	woGR	- (3.55)	- (6.29)	- (7.84)	- (0.23)	- (0.02)
	GR	+++ (613.77)	- (36.53)	+ (41.50)	- (0.59)	+ (53.37)
MSRGAN	woGR	++ (234.43)	+++ (551.26)	+++ (525.55)	+ (52.67)	- (1.40)
	wGR	+++ (626.46)	+++ (815.11)	+++ (831.35)	+ (79.40)	+ (35.04)

\* -: 0 ~ 20. +: 20 ~ 100. ++: 100 ~ 500. +++:  $\geq 500$ .

Table 1. Quantitative evaluations (CHI). There appears to be a spectrum (continuous transition) for the discriminability of DDR.

extracted features appear similar degradations as well. For blurred/noisy input images, the extracted feature maps also contain homologous blur/noise degradations.

**Effect of global residual.** In Sec. 5.1, we have revealed the importance and effectiveness of global residual (GR) for obtaining deep degradation representations for SR networks. But why GR is so important? What is the role of GR? Through visualization, we can provide a qualitative and intuitive explanation here. Comparing Fig. 10(a) and Fig. 10(b), it can be observed that by adopting GR, the extracted features seem to contain less components of original shape and content information. Thus, GR can help remove the redundant image content information and make the network concentrate more on obtaining features that are related to low-level degradation information.

**Effect of GAN.** Previously, we have discussed the difference between MSE-based and GAN-based SR methods in their deep representations. We find that GAN-based method can better obtain feature representations that are discriminative to different degradation types. As shown in Fig. 10(a) and Fig. 10(c), the feature maps extracted by GAN-based method contain less object shape and content information compared with MSE-based method. This partially explains why the deep representations of GAN-based method are more discriminative, even without global residual. Comparing Fig. 10(c) and Fig. 10(d), when there is global residual, the feature maps containing the image original content information are further reduced, leading to stronger discriminability to degradation types.

## 6. Inspirations and Future Work

Based on our discoveries, we draw significant inspirations on the future work. Due to the space limitation, more contents are shown in the supplementary file.

**Interpreting the Generalization of SR Networks.** In the previous sections, we have discussed the characteristics of DDR. Notably, the deep feature representations are obtained by super-resolution networks that are trained on clean dataset, i.e., the training data only contain downsampling degradation without blur or noise. What if we involve degraded data in the training process? To explore this question, we train a SRGAN-wGR model on noisy data (add Gaussian noise with  $\sigma = 20$  on LR inputs). Then we compare the representation difference between models trained on clean data and noisy data. As presented in Fig. 11, we observe that by incorporating degraded data into training, the SR model is capable of simultaneously performing restoration and super-resolution. From the aspect of features, if the model is trained only on clean data, the obtained feature representations show strong discriminability to clean data and noisy data; but if the model is trained on noisy data, such discriminability disappears. It suggests that by incorporating more degraded data into training, the model becomes robust to handle more degradation types, and the distributions of the deep representations of different degraded data become unanimous with that of clean data. This can partially explain and evaluate the generalization ability of different models in feature level.

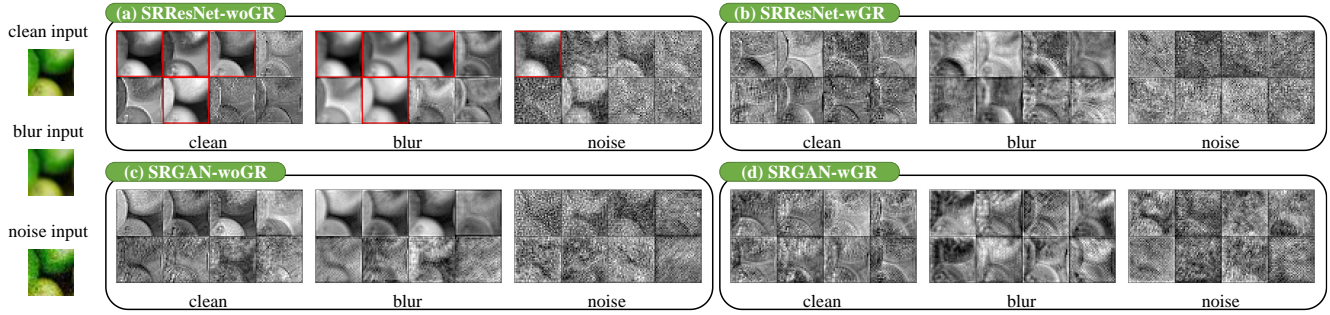


Figure 10. Visualization of feature maps. GR and GAN can facilitate the network to obtain more features on degradation information.

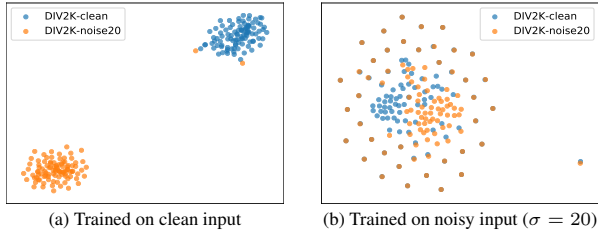


Figure 11. By incorporating more degraded data into training, the model becomes robust to handle more degradation types. Simultaneously, the distributions of the deep representations of different degraded data are more unanimous.

## 7. Conclusions

Can we find semantics in SR networks? Yes! In this paper, we have successfully discovered and interpreted the semantics of SR networks. Different from high-level vision networks, such semantics are highly related to the image degradation types and degrees. A series of observations and conclusions on the semantic representations in SR networks are drawn.

## References

- [1] Eirikur Agustsson and Radu Timofte. Ntire 2017 challenge on single image super-resolution: Dataset and study. In *The IEEE Conference on Computer Vision and Pattern Recognition (CVPR) Workshops*, July 2017.
- [2] Sefi Bell-Kligler, Assaf Shocher, and Michal Irani. Blind super-resolution kernel estimation using an internal-gan. *arXiv preprint arXiv:1909.06581*, 2019.
- [3] Tadeusz Caliński and Jerzy Harabasz. A dendrite method for cluster analysis. *Communications in Statistics-theory and Methods*, 3(1):1–27, 1974.
- [4] Kostadin Dabov, Alessandro Foi, Vladimir Katkovnik, and Karen Egiazarian. Image denoising by sparse 3-d transform-domain collaborative filtering. *IEEE Transactions on image processing*, 16(8):2080–2095, 2007.
- [5] Tao Dai, Jianrui Cai, Yongbing Zhang, Shu-Tao Xia, and Lei Zhang. Second-order attention network for single image super-resolution. In *Proceedings of the IEEE/CVF Conference on Computer Vision and Pattern Recognition*, pages 11065–11074, 2019.
- [6] Jeff Donahue, Yangqing Jia, Oriol Vinyals, Judy Hoffman, Ning Zhang, Eric Tzeng, and Trevor Darrell. Decaf: A deep convolutional activation feature for generic visual recognition. In *International conference on machine learning*, pages 647–655. PMLR, 2014.
- [7] Chao Dong, Chen Change Loy, Kaiming He, and Xiaoou Tang. Learning a deep convolutional network for image super-resolution. In *European conference on computer vision*, pages 184–199. Springer, 2014.
- [8] Chao Dong, Chen Change Loy, and Xiaoou Tang. Accelerating the super-resolution convolutional neural network. In *European conference on computer vision*, pages 391–407. Springer, 2016.
- [9] Jinjin Gu and Chao Dong. Interpreting super-resolution networks with local attribution maps. In *Proceedings of the IEEE/CVF Conference on Computer Vision and Pattern Recognition*, 2021.
- [10] Jinjin Gu, Hannan Lu, Wangmeng Zuo, and Chao Dong. Blind super-resolution with iterative kernel correction. In *Proceedings of the IEEE/CVF Conference on Computer Vision and Pattern Recognition*, pages 1604–1613, 2019.
- [11] Kaiming He, Xiangyu Zhang, Shaoqing Ren, and Jian Sun. Deep residual learning for image recognition. In *Proceedings of the IEEE conference on computer vision and pattern recognition*, pages 770–778, 2016.
- [12] Harold Hotelling. Analysis of a complex of statistical variables into principal components. *Journal of educational psychology*, 24(6):417, 1933.
- [13] W Ronny Huang, Zeyad Emam, Micah Goldblum, Liam Fowl, Justin K Terry, Furong Huang, and Tom Goldstein. Understanding generalization through visualizations. 2020.
- [14] Justin Johnson, Alexandre Alahi, and Li Fei-Fei. Perceptual losses for real-time style transfer and super-resolution. In *European conference on computer vision*, pages 694–711. Springer, 2016.
- [15] Robert Keys. Cubic convolution interpolation for digital image processing. *IEEE transactions on acoustics, speech, and signal processing*, 29(6):1153–1160, 1981.
- [16] Jiwon Kim, Jung Kwon Lee, and Kyoung Mu Lee. Accurate image super-resolution using very deep convolutional networks. In *Proceedings of the IEEE conference on computer vision and pattern recognition*, pages 1646–1654, 2016.
- [17] Alex Krizhevsky, Geoffrey Hinton, et al. Learning multiple layers of features from tiny images. 2009.

- [18] Ivan Laptev, Marcin Marszałek, Cordelia Schmid, and Benjamin Rozenfeld. Learning realistic human actions from movies. In *2008 IEEE Computer Society Conference on Computer Vision and Pattern Recognition CVPR 2008*, 2008.
- [19] Christian Ledig, Lucas Theis, Ferenc Huszár, Jose Caballero, Andrew Cunningham, Alejandro Acosta, Andrew Aitken, Alykhan Tejani, Johannes Totz, Zehan Wang, et al. Photo-realistic single image super-resolution using a generative adversarial network. In *Proceedings of the IEEE conference on computer vision and pattern recognition*, pages 4681–4690, 2017.
- [20] Seungmin Lee, Dongwan Kim, Namil Kim, and Seong-Gyun Jeong. Drop to adapt: Learning discriminative features for unsupervised domain adaptation. In *Proceedings of the IEEE/CVF International Conference on Computer Vision*, pages 91–100, 2019.
- [21] Bee Lim, Sanghyun Son, Heewon Kim, Seungjun Nah, and Kyoung Mu Lee. Enhanced deep residual networks for single image super-resolution. In *Proceedings of the IEEE conference on computer vision and pattern recognition workshops*, pages 136–144, 2017.
- [22] Anran Liu, Yihao Liu, Jinjin Gu, Yu Qiao, and Chao Dong. Blind image super-resolution: A survey and beyond. *arXiv preprint arXiv:2107.03055*, 2021.
- [23] Zhengxiong Luo, Y. Huang, Shang Li, Liang Wang, and T. Tan. Unfolding the alternating optimization for blind super resolution. *ArXiv*, abs/2010.02631, 2020.
- [24] Volodymyr Mnih, Koray Kavukcuoglu, David Silver, Andrei A Rusu, Joel Veness, Marc G Bellemare, Alex Graves, Martin Riedmiller, Andreas K Fiedjeland, Georg Ostrovski, et al. Human-level control through deep reinforcement learning. *nature*, 518(7540):529–533, 2015.
- [25] Aaron van den Oord, Yazhe Li, and Oriol Vinyals. Representation learning with contrastive predictive coding. *arXiv preprint arXiv:1807.03748*, 2018.
- [26] Mohammad Saeed Rad, Behzad Bozorgtabar, Urs-Viktor Marti, Max Basler, Hazim Kemal Ekenel, and Jean-Philippe Thiran. Srobb: Targeted perceptual loss for single image super-resolution. In *Proceedings of the IEEE/CVF International Conference on Computer Vision*, pages 2710–2719, 2019.
- [27] Ramprasaath R Selvaraju, Michael Cogswell, Abhishek Das, Ramakrishna Vedantam, Devi Parikh, and Dhruv Batra. Grad-cam: Visual explanations from deep networks via gradient-based localization. In *Proceedings of the IEEE international conference on computer vision*, pages 618–626, 2017.
- [28] Karen Simonyan, Andrea Vedaldi, and Andrew Zisserman. Deep inside convolutional networks: Visualising image classification models and saliency maps. *arXiv preprint arXiv:1312.6034*, 2013.
- [29] Laurens Van der Maaten and Geoffrey Hinton. Visualizing data using t-sne. *Journal of machine learning research*, 9(11), 2008.
- [30] Petar Veličković, Guillem Cucurull, Arantxa Casanova, Adriana Romero, Pietro Lio, and Yoshua Bengio. Graph attention networks. *arXiv preprint arXiv:1710.10903*, 2017.
- [31] Longguang Wang, Yingqian Wang, Xiaoyu Dong, Qingyu Xu, Jungang Yang, Wei An, and Yulan Guo. Unsupervised degradation representation learning for blind super-resolution. In *Proceedings of the IEEE/CVF Conference on Computer Vision and Pattern Recognition*, pages 10581–10590, 2021.
- [32] Xintao Wang, Ke Yu, Shixiang Wu, Jinjin Gu, Yihao Liu, Chao Dong, Yu Qiao, and Chen Change Loy. Esrgan: Enhanced super-resolution generative adversarial networks. In *European Conference on Computer Vision Workshops*, pages 63–79. Springer, 2018.
- [33] Yang Wang, Yang Cao, Zheng-Jun Zha, Jing Zhang, and Zhiwei Xiong. Deep degradation prior for low-quality image classification. In *Proceedings of the IEEE/CVF Conference on Computer Vision and Pattern Recognition*, pages 11049–11058, 2020.
- [34] Yandong Wen, Kaipeng Zhang, Zhifeng Li, and Yu Qiao. A discriminative feature learning approach for deep face recognition. In *European conference on computer vision*, pages 499–515. Springer, 2016.
- [35] Jianchao Yang, John Wright, Thomas Huang, and Yi Ma. Image super-resolution as sparse representation of raw image patches. In *2008 IEEE conference on computer vision and pattern recognition*, pages 1–8. IEEE, 2008.
- [36] Jianchao Yang, John Wright, Thomas S Huang, and Yi Ma. Image super-resolution via sparse representation. *IEEE transactions on image processing*, 19(11):2861–2873, 2010.
- [37] Yuan Yuan, Siyuan Liu, Jiawei Zhang, Yongbing Zhang, Chao Dong, and Liang Lin. Unsupervised image super-resolution using cycle-in-cycle generative adversarial networks. In *CVPRW*, pages 701–710, 2018.
- [38] Tom Zahavy, Nir Ben-Zrihem, and Shie Mannor. Graying the black box: Understanding dqns. In *International Conference on Machine Learning*, pages 1899–1908. PMLR, 2016.
- [39] Matthew D Zeiler and Rob Fergus. Visualizing and understanding convolutional networks. In *European conference on computer vision*, pages 818–833. Springer, 2014.
- [40] Matthew D Zeiler, Dilip Krishnan, Graham W Taylor, and Rob Fergus. Deconvolutional networks. In *2010 IEEE Computer Society Conference on computer vision and pattern recognition*, pages 2528–2535. IEEE, 2010.
- [41] Kai Zhang, Wangmeng Zuo, Yunjin Chen, Deyu Meng, and Lei Zhang. Beyond a gaussian denoiser: Residual learning of deep cnn for image denoising. *IEEE transactions on image processing*, 26(7):3142–3155, 2017.
- [42] Wenlong Zhang, Yihao Liu, Chao Dong, and Yu Qiao. Ranksrgan: Generative adversarial networks with ranker for image super-resolution. In *Proceedings of the IEEE/CVF International Conference on Computer Vision*, pages 3096–3105, 2019.
- [43] Yulun Zhang, Kunpeng Li, Kai Li, Lichen Wang, Bineng Zhong, and Yun Fu. Image super-resolution using very deep residual channel attention networks. In *Proceedings of the European conference on computer vision (ECCV)*, pages 286–301, 2018.
- [44] Yu Zhang, Peter Tiño, Aleš Leonardis, and Ke Tang. A survey on neural network interpretability. *arXiv preprint arXiv:2012.14261*, 2020.

- [45] Bolei Zhou, Aditya Khosla, Agata Lapedriza, Aude Oliva, and Antonio Torralba. Learning deep features for discriminative localization. In *Proceedings of the IEEE conference on computer vision and pattern recognition*, pages 2921–2929, 2016.



# Discovering “Semantics” in Super-Resolution Networks

## Supplementary File

Yihao Liu<sup>1 2\*</sup> Anran Liu<sup>1 4\*</sup> Jinjin Gu<sup>1 5</sup>  
Zhipeng Zhang<sup>2 6</sup> Wenhao Wu<sup>7</sup> Yu Qiao<sup>1 3</sup> Chao Dong<sup>1†</sup>  
<sup>1</sup>Shenzhen Institute of Advanced Technology, CAS  
<sup>2</sup>University of Chinese Academy of Sciences  
<sup>3</sup>Shanghai AI Lab <sup>4</sup>The University of Hongkong  
<sup>5</sup>University of Sydney <sup>6</sup>Institute of Automation, CAS <sup>7</sup>Baidu Inc.

### Abstract

*In this supplementary file, we provide more supporting materials. First, we introduce more background knowledge on the deep semantic representations of high-level and low-level vision networks. Then, we make a comparison between classification and super-resolution networks, in terms of problem formulations and network architectures. The experimental implementation details of the main paper are described as well. We also detail the numerical definitions of the adopted quantitative indicators (i.e., WD, BD and CHI). Further, for better comparison, we design a unified backbone framework to support and validate our findings in the main paper. There are also more discussions in this file.*

### 1. Background

Since the emergence of deep convolutional neural network (CNN), a large number of computer vision tasks have been drastically promoted, including high-level vision tasks such as image classification [48, 56, 19, 23, 22], object localization [46, 18, 45] and semantic segmentation [37, 3, 6, 64], as well as low-level vision tasks such as image super-resolution [12, 32, 65, 74, 7], denoising [72, 73, 15, 44], dehazing [4, 71, 14, 9], etc. However, an interesting phenomenon is that even if we have successfully applied CNNs to many tasks, yet we still do not have a thorough understanding of its intrinsic working mechanism.

To better understand the behaviors of CNN, many efforts have been put in the neural network interpretability for *high-level vision* [55, 49, 69, 50, 41, 27, 39, 77, 1]. Most of them attempt to interpret the CNN decisions by visualization techniques, such as visualizing the interme-

diate feature maps (or saliency maps and class activation maps) [55, 69, 1, 78, 50], computing the class notion images which maximize the class score [55], or projecting feature representations [67, 66, 79, 24]. For high-level vision tasks, especially image classification, researchers have established a set of techniques for interpreting deep models and have built up a preliminary understanding of CNN behaviors [16]. One representative work is done by Zeiler et al. [69], who reveal the hierarchical nature of CNN by visualizing and interpreting the feature maps: the shallow layers respond to low-level features such as corners, curves and other edge/color conjunctions; the middle layers capture more complex texture combinations; the deeper layers are learned to encode more abstract and class-specific patterns, e.g., faces and legs. These patterns can be well interpreted by human perception and help partially explain the CNN decisions for high-level vision tasks.

As for *low-level vision* tasks, however, similar research work is absent. The possible reasons are as follows. In high-level vision tasks, there are usually artificially predefined semantic labels/categories. Thus, we can intuitively associate feature representations with these labels. Nevertheless, in low-level vision tasks, there is no explicit predefined semantics, making it hard to map the representations into a domain that the human can make sense of. Further, high-level vision usually performs *classification* in a discrete target domain with distinct categories, while low-level vision aims to solve a *regression* problem with continuous output values. Hence, without the guidance of predefined category semantics, it seems not so straightforward to interpret low-level vision networks.

In this paper, we take super-resolution (SR), one of the most representative tasks in low-level vision, as research object. Previously, it is generally thought that the features extracted from the SR network have no specific “semantic” information, and the network simply learns some complex

\*The first two authors contributed equally (co-first authors). Email: liuyihao14@mails.ucas.ac.cn, liuar616@connect.hku.hk.

†Corresponding author. Email: chao.dong@siat.ac.cn.

non-linear functions to model the relations between network input and output. Are CNN features SR networks really in lack of any semantics? Can we find any kind of “semantics” in SR networks? In this paper, we aim to give an answer to these questions. We reveal that there **are** semantics existing in SR networks. We first discover and interpret the “semantics” of deep representations in SR networks. But different from high-level vision networks, such semantics relate to the image degradation types and degrees. Accordingly, we designate the deep semantic representations in SR networks as deep degradation representations (DDR).

## 2. Classification vs. Super-resolution

### 2.1. Formulation

**Classification.** Classification aims to categorize an input image  $X$  into a discrete object class:

$$\hat{Y} = G_{CL}(X), \quad (1)$$

where  $G_{CL}$  represents the classification network, and  $\hat{Y} \in \mathbb{R}^C$  is the predicted probability vector indicating which of the  $C$  categories  $X$  belongs to. In practice, cross-entropy loss is usually adopted to train the classification network:

$$CE(Y, \hat{Y}) = - \sum_{i=1}^C y_i \log \hat{y}_i, \quad (2)$$

where  $Y \in \mathbb{R}^C$  is a one-hot vector representing the ground-truth class label.  $\hat{y}_i$  is the  $i$ -th row element of  $\hat{Y}$ , indicating the predicted probability that  $X$  belongs to the  $i$ -th class.

**Super-resolution.** A general image degradation process can be model as follows:

$$X = (Y \otimes k) \downarrow_s + n, \quad (3)$$

where  $Y$  is the high-resolution (HR) image and  $\otimes$  denotes the convolution operation.  $X$  is the degraded high-resolution (LR) image. There are three types of degradation in this model: blur kernel  $k$ , downsampling operation  $\downarrow_s$  and additive noise  $n$ . Hence, super-resolution can be regarded as a superset of other restoration tasks like denoising and deblurring.

Super-resolution (SR) is the inverse problem of Equ. (3). Given the input LR image  $X \in \mathbb{R}^{M \times N}$ , the super-resolution network attempts to produce its HR version:

$$\hat{Y} = G_{SR}(X), \quad (4)$$

where  $G_{SR}$  represents the super-resolution network,  $\hat{Y} \in \mathbb{R}^{sM \times sN}$  is the predicted HR image and  $s$  is the upscaling factor. This procedure can be regarded as a typical regression task. At present, there are two groups of method: **MSE-based** and **GAN-based** methods. The former one

treats SR as a reconstruction problem, which utilizes pixel-wise loss such as  $L_2$  loss to achieve high PSNR values.

$$L_2(Y, \hat{Y}) = \frac{1}{r^2 NM} \sum_{i=1}^{rN} \sum_{j=1}^{rM} \|Y_{i,j} - \hat{Y}_{i,j}\|_2^2. \quad (5)$$

This is the most widely used loss function in many image restoration tasks [12, 36, 75, 73, 4, 17]. However, such loss tends to produce over-smoothed images. To generate photo-realistic SR results, the latter method incorporates adversarial learning and perceptual loss to benefit better visual perception. The optimization is expressed as following min-max problem:

$$\begin{aligned} \min_{\theta_{G_{SR}}} \max_{\theta_{D_{SR}}} & \mathbb{E}_{Y \sim p_{HR}} [\log D_{SR}(Y)] \\ & + \mathbb{E}_{X \sim p_{LR}} [\log(1 - D_{SR}(G_{SR}(X)))]. \end{aligned} \quad (6)$$

In such adversarial learning, a discriminator  $D_{SR}$  is introduced to distinguish super-resolved images from real HR images. Then, the generator loss is defined as:

$$L_G = -\log D_{SR}(G_{SR}(X)). \quad (7)$$

From the formulation, we can clearly see that image classification and image super-resolution represent two typical tasks in machine learning: classification and regression. The output of the classification task is discrete, while the output of the regression task is continuous.

### 2.2. Architectures

Due to the different output types, the CNN architectures of classification and super-resolution networks also differ. Generally, classification networks often contain multiple downsampling layers (e.g., pooling and strided convolution) to gradually reduce the spatial resolution of feature maps. After several convolutional and downsampling layers, there may be one or more fully-connected layers to aggregate global semantic information and generate a vector containing  $C$  elements. For the output layer, the SoftMax operator is frequently used to normalize the previously obtained vector into a probabilistic representation. Some renowned classification network structures include AlexNet [30], VGG [56], ResNet [19], InceptionNet [58, 25, 57], DenseNet [23], SENet[3], etc.

Unlike classification networks, super-resolution networks usually do not rely on downsampling layers, but upsampling layers (e.g., bilinear upsampling, transposed convolution [70] or subpixel convolution [54]). Thus, the spatial resolution of feature maps would increase. Another difference is that the output of the SR network is a three-channel image, rather than an abstract probability vector. The well-known SR network structures include SRCNN [12], FSRCNN [13], SRResNet [32], RDN [76], RCAN

[75], etc. An intuitive comparison of classification and SR networks in CNN architecture is shown in Fig. 6. We can notice that one is gradually downsampling, and the other is gradually upsampling, which displays the discrepancy between high-level vision and low-level vision tasks in structure designing.

Although there are several important architectural differences, classification networks and SR networks can share and adopt some proven effective building modules, like skip connection [19, 36] and attention mechanism[22, 75].

### 3. Implementation Details

In the main paper, we conduct experiments on ResNet18 [19] and SRResNet/ SRGAN [32]. We elaborate more details on the network structures and training settings here.

For ResNet18, we directly adopt the network structure depicted in [19]. Cross-entropy loss (Eq. 2) is used as the loss function. The learning rate is initialized to 0.1 and decreased with a cosine annealing strategy. We apply SGD optimizer with weight decay  $5 \times 10^{-4}$ . The trained model yields an accuracy of 92.86% on CIFAR10 testing set which consists of 10,000 images.

For SRResNet-wGR/SRResNet-woGR, we stack 16 residual blocks (RB) as shown in Fig. 3 of the main paper. The residual block is the same as depicted in [65], in which all the BN layers are removed. Two Pixel-shuffle layers [54] are utilized to conduct upsampling in the network, while the global residual branch is upsampled by bilinear interpolation.  $L_1$  loss is adopted as the loss function. The learning rate is initialized to  $2 \times 10^{-4}$  and is halved at [100k, 300k, 500k, 600k] iterations. A total of 600,000 iterations are executed.

For SRGAN-wGR/SRGAN-woGR, the generator is the same as SRResNet-wGR/SRResNet-woGR. The discriminator is designed as in [32]. Adversarial loss (Eq. 7) and perceptual loss [26] are combined as the loss functions, which are kept the same as in [32]. The learning rate of both generator and discriminator is initialized to  $1 \times 10^{-4}$  and is halved at [50k, 100k, 200k, 300k] iterations. A total of 600,000 iterations are executed. For all the super-resolution networks, we apply Adam optimizer [29] with  $\beta_1 = 0.9$  and  $\beta_2 = 0.99$ . All the training LR patches are of size  $128 \times 128$ . When testing,  $32 \times 32$  patches are fed into the networks to obtain deep features. In practice, we find that the patch size has little effect on revealing the deep degradation representations.

All above models are trained on PyTorch platform with GeForce RTX 2080 Ti GPUs.

### 4. Definitions of WD, BD and CHI

In Sec. 3.1 of the main paper, we describe the adopted analysis method on deep feature representations. Many

other literatures also have adopted similar approaches to interpret and visualize the deep models, such as Graph Attention Network [63], Recurrent Networks [27], Deep Q-Network [68] and Neural Models in NLP [35]. Most aforementioned researches adopt t-SNE as a qualitative analysis technique. To better illustrate and quantitatively measure the semantic discriminability of deep feature representations, we take a step further and introduce several indicators, which are originally used to evaluate the clustering performance, according to the data structure after dimensionality reduction by t-SNE. Specifically, we propose to adopt within-cluster dispersion (WD), between-clusters dispersion (BD) and Calinski-Harabaz Index (CHI) [5] to provide some rough yet practicable quantitative measures for reference. For  $K$  clusters, WD, BD and CHI are defined as:

$$WD(K) = \sum_{k=1}^K \sum_{i=1}^{n(k)} \|\mathbf{x}_k^i - \bar{\mathbf{x}}_k\|^2, \quad (8)$$

where  $\mathbf{x}_k^i$  represents the  $i$ -th datapoint belonging to class  $k$  and  $\bar{\mathbf{x}}_k$  is the average mean of all  $n(k)$  datapoints that belong to class  $k$ . Datapoints belonging to the same class should be close enough to each other and WD measures the compactness within a cluster.

$$BD(K) = \sum_{k=1}^K n(k) \|\bar{\mathbf{x}}_k - \bar{\mathbf{x}}\|^2, \quad (9)$$

where  $\bar{\mathbf{x}}$  represents the average mean of all datapoints. BD measures the distance between clusters. Intuitively, larger BD value indicates stronger discriminability between different feature clusters. Given  $K$  clusters and  $N$  datapoints in total ( $N = \sum_k n(k)$ ), by combining WD and BD, the CHI is formulated as:

$$CHI(K) = \frac{BD(K)}{WD(K)} \cdot \frac{(N - K)}{(K - 1)}. \quad (10)$$

It is represented as the ratio of the between-clusters dispersion mean and the within-cluster dispersion. The CHI score is higher when clusters are dense and well separated, which relates to a standard concept of a cluster.

### 5. Understanding and Evaluating Deep Feature Representations

In this section, we adopt quantitative indicators to help evaluate the deep representations. From Fig. 1, it can be observed that as the network deepens, the extracted feature representations produce obvious clusters, i.e., the learned features are increasingly becoming semantically discriminative. Further, such discriminative semantics are coherent with the artificially predefined labels (semantic categories). This is an intuitive and natural observation on which lots of representation and discriminative learning methods were

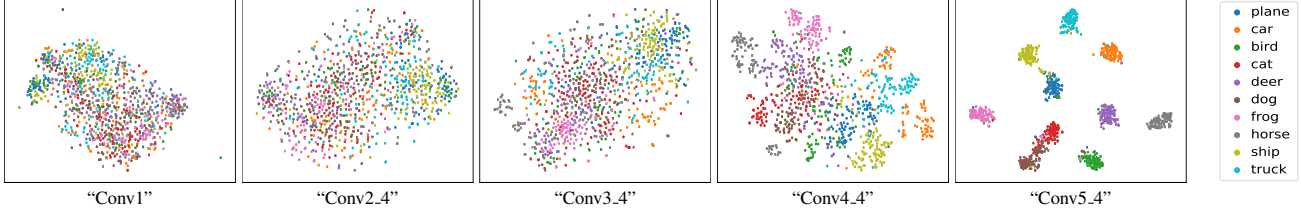


Figure 1. Projected feature representations extracted from different layers of ResNet18 using t-SNE. With the network deepens, the representations become more discriminative to object categories, which clearly shows the semantics of the representations in classification.

#Layer	Conv1	Conv2_4	Conv3_4	Conv4_4	Conv5_4
Dim	$64 \times 32 \times 32$	$64 \times 32 \times 32$	$128 \times 16 \times 16$	$256 \times 8 \times 8$	$512 \times 4 \times 4$
WD $\downarrow (\times 10^5)$	$4.07 \pm 0.43$	$3.41 \pm 0.31$	$3.32 \pm 0.31$	$2.06 \pm 0.13$	$0.71 \pm 0.06$
BD $\uparrow (\times 10^5)$	$1.04 \pm 0.13$	$1.22 \pm 0.11$	$1.84 \pm 0.40$	$5.77 \pm 0.23$	$10.74 \pm 0.20$
CHI $\uparrow$	$28.18 \pm 1.69$	$39.22 \pm 1.44$	$61.12 \pm 13.62$	$309.31 \pm 31.10$	$1688.62 \pm 145.15$

Table 1. Quantitative measures for the discriminability of the projected deep feature representations. We statistically report the mean value and the standard deviation of each metric. The adopted indicators well reflect the effect of feature clustering quantitatively.

based [67, 43, 34, 66]. Note that the class labels in the scatterplots are only used to assign a color/symbol to the datapoints for better visualization. The class information is not used by t-SNE to determine the spatial coordinates of the data after dimension reduction.

Since the class label of each datapoint is available, we can calculate the WD, BD and CHI scores for each projected map derived from t-SNE. The results are summarized in Tab. 1. It is remarkable that by introducing these indices, we can now quantitatively assess the semantic discriminability of feature representations. Combining Fig. 1 and Tab. 1, it is observed that the quantitative results are consistent with the previous qualitative analysis. With the increase of network depth, the feature representations are more semantically discriminative, coinciding with predefined class labels.

In the main paper, we mainly report the CHI scores. Here we provide the complete quantitative results in Tab. 1, Tab. 2 and Tab. 3. It can be observed that the qualitative visualization results (Fig. 2 and Fig. 3) are in accordance with the quantitative results. By introducing the quantitative measures, we now can better evaluate the semantic discriminability of deep feature representations.

**Rationality of Using Quantitative Measures with t-SNE.** Notably, t-SNE is not a numerical technique but a probabilistic one. It minimizes the Kullback-Leibler (KL) divergence between the distributions that measure pairwise similarities of the input high-dimensional data and that of the corresponding low-dimensional points in the embedding. Further, t-SNE is a non-convex optimization process which is performed using a gradient descent method, as a result of which several optimization parameters need to be chosen, like perplexity, iterations and learning rate. Hence, the reconstruction solutions may differ due to the choice of

different optimization parameters and the initial random states. In this paper, we used exactly the same optimization procedure for all experiments. Moreover, we conduct extensive experiments using different parameters and demonstrate that the quality of the optima does not vary much from run to run, which is also emphasized in the t-SNE paper. To make the quantitative analysis more statistically solid, for each projection process, we run t-SNE five times and report the average and standard deviations of every metric.

## 6. Visualization of Feature Maps

In the main paper, we have displayed the feature maps of each SR network to make a qualitative interpretation about the formation of deep degradation representations. However, due to space limitation, we only display 8 feature maps with the largest eigenvalues. Since there are 64 channels in the “ResBlock16” layer, we here provide the complete 64 feature maps of each input, as shown in Fig. 4. The visualization results reveal that global residual (GR) and adversarial learning (GAN) can facilitate the network to concentrate more on the degradation information instead of image content information. For the same degradation type, the extracted feature maps are close to each other, while the feature maps of different degradation types are very different.

## 7. Exploration of Network Structure

In the main paper, we choose ResNet18 [19] and SRResNet/ SRGAN [32] as the backbones of classification and SR networks, respectively. In order to eliminate the influence of different network structures, we design a unified backbone framework, which is composed of the same basic building modules but connected with different tails for downsampling and upsampling to conduct classification and super-



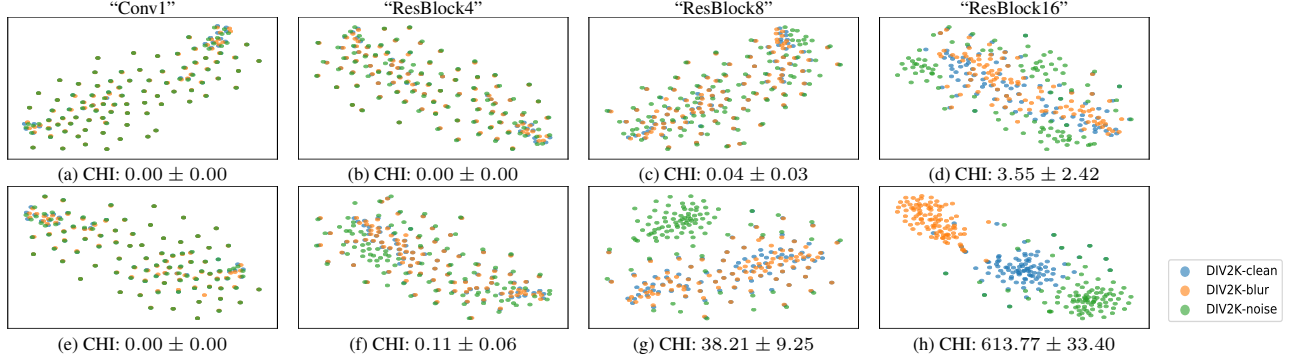


Figure 2. Projected feature representations extracted from different layers of SRResNet-woGR (1st row) and SRResNet-wGR (2nd row) using t-SNE. With image global residual (GR), the representations of MSE-based SR networks show discriminability to degradation types.

SRResNet-woGR				
#Layer	Conv1	ResBlock4	ResBlock8	ResBlock16
WD↓( $\times 10^4$ )	$8.35 \pm 0.14$	$8.90 \pm 0.22$	$9.28 \pm 0.31$	$4.98 \pm 0.48$
BD↑	$0.29 \pm 0.14$	$1.98 \pm 1.47$	$25.60 \pm 17.73$	$1149.20 \pm 765.12$
CHI↑	$0.00 \pm 0.00$	$0.00 \pm 0.00$	$0.04 \pm 0.03$	$3.55 \pm 2.42$
SRResNet-wGR				
#Layer	Conv1	ResBlock4	ResBlock8	ResBlock16
WD↓( $\times 10^4$ )	$8.20 \pm 0.18$	$8.40 \pm 0.09$	$4.40 \pm 0.50$	$0.86 \pm 0.11$
BD↑	$0.48 \pm 0.34$	$62.74 \pm 33.99$	$11096.79 \pm 2051.02$	$35470.66 \pm 4412.66$
CHI↑	$0.00 \pm 0.00$	$0.11 \pm 0.06$	$38.21 \pm 9.25$	$613.77 \pm 33.40$

Table 2. Quantitative measures for the projected deep feature representations obtained by SRResNet-woGR and SRResNet-wGR.

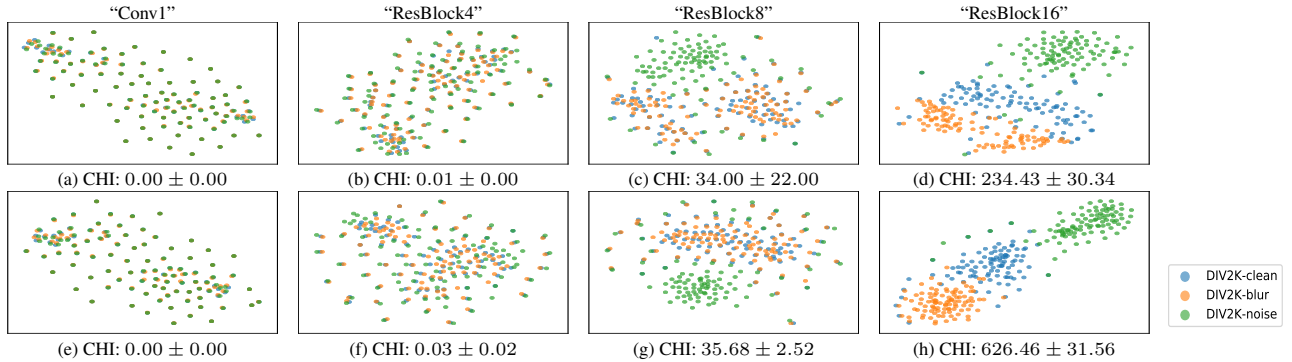
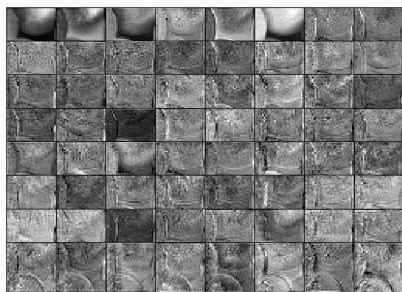


Figure 3. Projected feature representations extracted from different layers of SRGAN-woGR (1st row) and SRGAN-wGR (2nd row) using t-SNE. Even without GR, GAN-based SR networks can still obtain deep degradation representations.

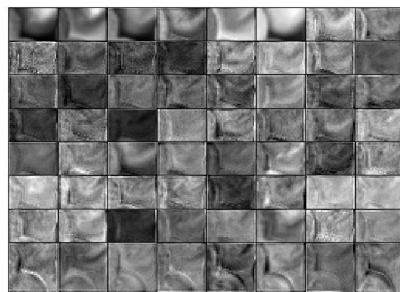
SRGAN-woGR				
#Layer	Conv1	ResBlock4	ResBlock8	ResBlock16
WD↓( $\times 10^4$ )	$7.94 \pm 0.20$	$7.83 \pm 0.33$	$4.65 \pm 0.58$	$1.44 \pm 0.28$
BD↑	$0.58 \pm 0.41$	$4.79 \pm 2.43$	$9809.00 \pm 4501.19$	$22459.35 \pm 3560.33$
CHI↑	$0.00 \pm 0.00$	$0.01 \pm 0.00$	$34.00 \pm 22.00$	$234.43 \pm 30.34$
SRGAN-wGR				
#Layer	Conv1	ResBlock4	ResBlock8	ResBlock16
WD↓( $\times 10^4$ )	$7.47 \pm 0.20$	$7.97 \pm 0.19$	$4.83 \pm 0.52$	$0.72 \pm 0.10$
BD↑	$0.41 \pm 0.36$	$14.89 \pm 8.85$	$11600.91 \pm 1424.10$	$30180.52 \pm 2884.65$
CHI↑	$0.00 \pm 0.00$	$0.03 \pm 0.02$	$35.68 \pm 2.52$	$626.46 \pm 31.56$

Table 3. Quantitative measures for the projected deep feature representations obtained by SRGAN-woGR and SRGAN-wGR.

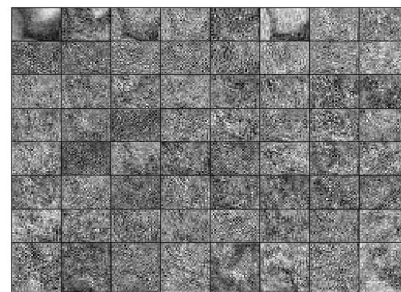
(a) SRResNet-woGR



clean

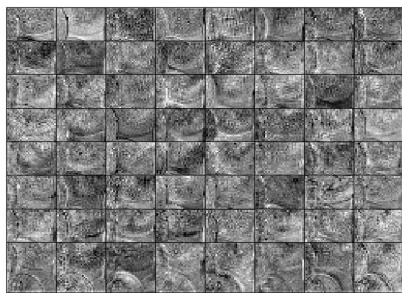


blur

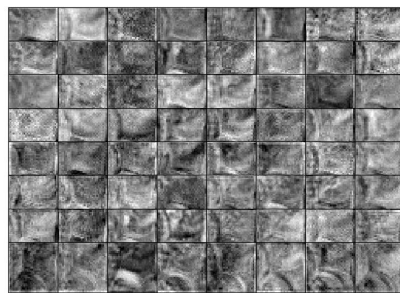


noise

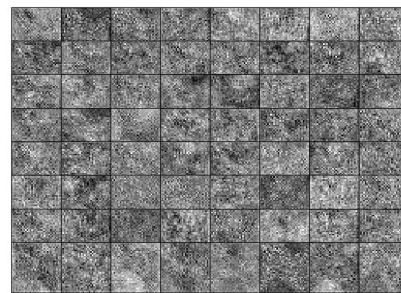
(b) SRResNet-wGR



clean



blur

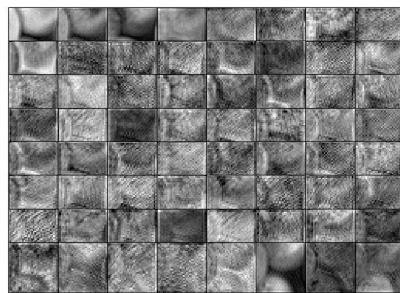


noise

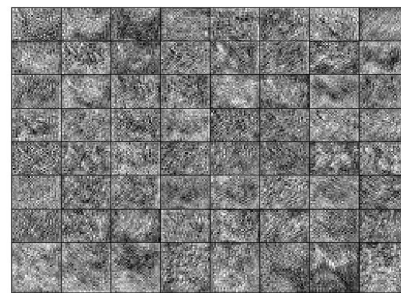
(c) SRGAN-woGR



clean



blur

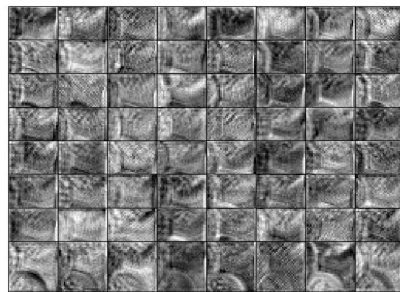


noise

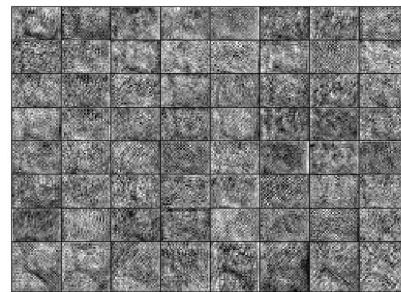
(d) SRGAN-wGR



clean



blur



noise

Figure 4. Visualization of feature maps. GR and GAN can facilitate the network to obtain more features on degradation information.

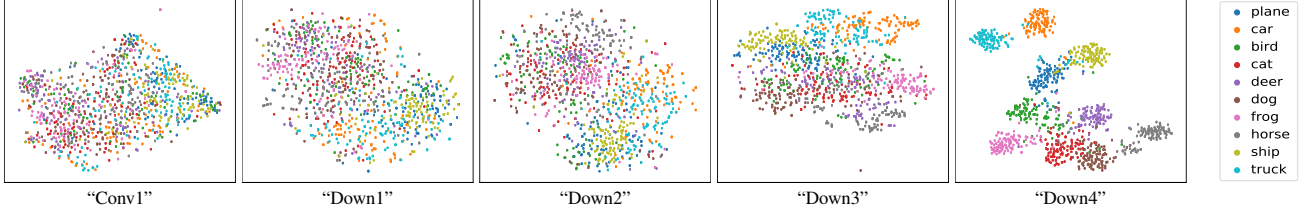


Figure 5. Projected feature representations extracted from different layers of unified backbone framework (classification) using t-SNE. The results are similar to ResNet18, which validates that the deep semantic representations are uncorrelated with network structures but are associated with the task itself.

#Layer	Conv1	Down1	Down2	Down3	Down4
Dim	$64 \times 32 \times 32$	$64 \times 32 \times 32$	$128 \times 16 \times 16$	$256 \times 8 \times 8$	$512 \times 4 \times 4$
WD $\downarrow (\times 10^5)$	$3.64 \pm 0.33$	$2.76 \pm 0.27$	$2.52 \pm 0.19$	$1.83 \pm 0.05$	$0.59 \pm 0.02$
BD $\uparrow (\times 10^5)$	$1.10 \pm 0.13$	$0.97 \pm 0.18$	$1.60 \pm 0.19$	$3.84 \pm 0.40$	$7.48 \pm 0.32$
CHI $\uparrow$	$33.11 \pm 1.38$	$39.53 \pm 9.98$	$70.11 \pm 9.94$	$230.95 \pm 22.63$	$1403.96 \pm 27.17$

Table 4. Quantitative measures for the discriminability of the projected deep feature representations obtained by unified backbone framework (classification).

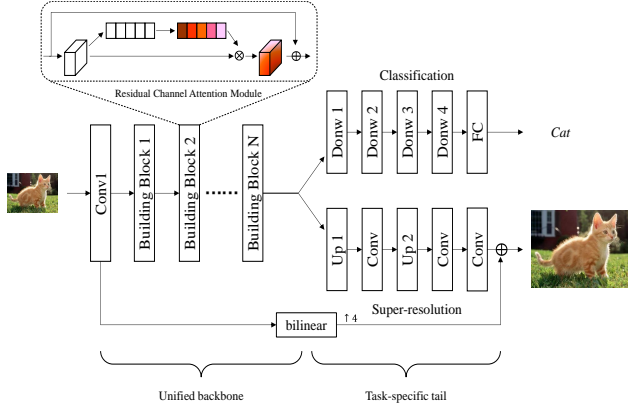


Figure 6. Unified backbone framework for classification and super-resolution. The two networks share the same backbone structure and different tails. We adopt channel attention module as the basic building block in the backbone.  $\otimes$  denotes element-wise multiplication.

resolution respectively.

The unified architecture is shown in Fig. 6. To differ from the residual block in the main paper, we adopt residual channel attention layer as basic building block, which is inspired by SENet [22] and RCAN [75]. For classification, the network tail consists of three maxpooling layers and a fully connected layer; for super-resolution, the network tail consists of two pixel-shuffle layers to upsample the feature maps. According to the conclusions in the main paper, we adopt global residual (GR) in the network design to obtain deep degradation representations (DDR). Except the network structure, all the training protocols are kept the same as in the main paper. The training details are the same

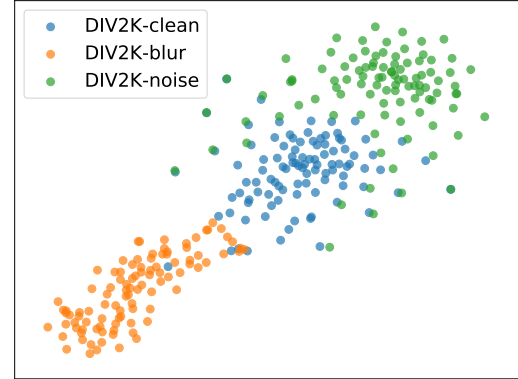


Figure 7. Projected feature representations extracted from unified backbone framework (super-resolution) using t-SNE.

as depicted in Sec. 3. After training, the unified backbone framework for classification yields an accuracy of 92.08% on CIFAR10 testing set.

The experimental results are shown in Fig. 5, Fig. 7 and Tab. 4. From the results, we can see that the observations are consistent with the findings in the main paper. It suggests that the semantic representations do not stem from network structures, but from the task itself. Hence, our findings are not only limited to specific structures but are universal.

## 8. Discussions on Dimensionality Reduction

Among the numerous dimensionality reduction techniques (e.g., PCA [21], CCA [8], LLE [47], Isomap[59], SNE[20]), t-Distributed Stochastic Neighbor Embedding (t-SNE) [62] is a widely-used and effective algorithm. It can



#Layer	Conv5_4					
Input #Dim	$512 \times 4 \times 4$					
Method	PCA(50)+t-SNE(2)	PCA(50)+t-SNE(3)	PCA	PCA	PCA	PCA
Reduced #Dim	2	3	2	3	4	5
WD $\downarrow (\times 10^5)$	$0.71 \pm 0.06$	$0.24 \pm 0.06$	0.19	0.32	0.39	0.47
BD $\uparrow (\times 10^5)$	$10.74 \pm 0.20$	$2.09 \pm 0.04$	1.27	1.61	1.95	2.24
CHI $\uparrow$	$1688.62 \pm 145.15$	$978.58 \pm 224.77$	729.64	562.85	554.92	526.64

Table 5. Quantitative comparison with dimensionality reduction methods and reduced dimensions. To utilize t-SNE, we first use PCA to pre-reduce the features to 50 dimensions. Since PCA is a numerical method, the result is fixed. For t-SNE, we report the mean and standard deviation for 5 runs. The quantitative results show that t-SNE surpasses PCA and reducing to two dimensions is better. The features are obtained by “Conv5\_4” layer of ResNet18.

greatly capture the local structure of the high-dimensional data and simultaneously reveal global structure such as the presence of clusters at several scales. Following [11, 40, 67, 68, 63, 66, 24], we also take advantage of the superior manifold learning capability of t-SNE for feature projection and visualization.

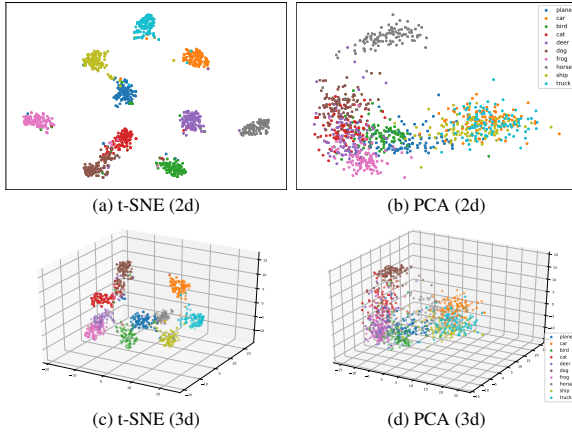


Figure 8. Comparison between PCA and t-SNE for projecting feature representations (“Conv5\_4” layer of ResNet18).

In this section we further explain the effectiveness of adopting t-SNE and why we choose to project high-dimensional features into two-dimensional datapoints. We first compare the projection results of PCA and t-SNE. From the results shown in Fig. 8, it can be observed that the projected features by t-SNE are successfully clustered together according to the semantic labels, while the projected features by PCA are not well separated. It is because that PCA is a linear dimension reduction method which cannot deal with complex non-linear data obtained by the neural networks. Thus, t-SNE is a better choice to conduct dimension reduction on CNN features. This suggests the effectiveness of t-SNE for the purpose of feature projection. Note that we do not claim t-SNE is the optimal or the best choice for dimensionality reduction. We just utilize t-SNE as a rational tool to show the trend behind deep representations, since t-SNE has been proven effective and practical

in our experiments and other literatures.

Then, we discuss the dimensions to reduce. We conduct dimensionality reduction to different dimensions. Since the highest dimension supported by t-SNE is 3, we first compare the effect between the two-dimensional projected features and the three-dimensional projected features by t-SNE. The qualitative and quantitative results are shown in Fig. 8 and Tab. 5. When we reduce the features to three dimensions, the reduced representations also show discriminability to semantic labels. However, quantitative results show that two dimensions can better portray the discriminability than three or higher dimensions. For PCA, the results are similar. With higher dimensions, the discriminability decrease. Hence, it is reasonable to reduce high-dimensional features into two-dimensional datapoints. Such settings are also adopted in [11, 66, 63, 24], which are proven effective.

## 9. Samples of Different Datasets

In the main paper, we adopt several different datasets to conduct experiments. Fig. 9 displays some example images from these datasets.

(a) DIV2K-clean: the original DIV2K [2] dataset. The high-resolution (HR) ground-truth (GT) images have 2K resolution and are of high visual quality. The low-resolution (LR) input images are downsampled from HR by bicubic interpolation, without any further degradations.

(b) DIV2K-noise: adding Gaussian noises to DIV2K-clean LR input, thus making it contain extra noise degradation. DIV2K-noise20 means the additive Gaussian noise level  $\sigma$  is 20, where the number denotes the noise level.

(c) DIV2K-blur: applying Gaussian blur to DIV2K-clean LR input, thus making it contain extra blur degradation. DIV2K-blur4 means the Gaussian blur width is 4.

(d) DIV2K-mild: officially synthesized from DIV2K [2] dataset as challenge dataset [60, 61], which contains noise, blur, pixel shifting and other degradations. The degradation modelling is unknown to challenge participants.

(e) Hollywood100: 100 images selected from Holly-



wood dataset [31], containing real-world old film frames with unknown degradations, which may have compression, noise, blur and other real-world degradations.

Dataset (a), (b), (c) and (d) have the same image contents but different degradations. However, we find that the deep degradation representations (DDR) obtained by SR networks have discriminability to these degradation types, even if the network has not seen these degradations at all during training. Further, for real-world degradation like in (e), the DDR are still able to discern it.

## 10. Inspirations and Future Work

### 10.1. Developing Degradation-adaptive Algorithms

One big challenge for image restoration is that there are myriad real-world and complicated cases with various degradation types and degrees. Thus, it is non-trivial to design a robust algorithm that can successfully handle all circumstances. One key to solve this problem is to make the algorithm be degradation-adaptive, so that it can specifically deal with different degradations.

In this paper, we have discovered the deep degradation representations in super-resolution networks, which are discriminative to different degradation types and degrees. This naturally provides the insight to solve the problem of blind restoration, where the profile of the degradation modeling is unknown and inaccessible. Concretely, we can leverage the deep degradation representations as prior knowledge to guide the subsequent modules to perform degradation-aware and degradation-adaptive processes.

### 10.2. Disentanglement of Image Content and Degradation

In plenty of image editing and synthesizing tasks, researchers seek to disentangle an image through different attributes, so that the image can be finely edited [28, 38, 10, 33, 42]. For example, semantic face editing [51, 52, 53] aims at manipulating facial attributes of a given image, e.g., pose, gender, age, smile, etc. Most methods attempt to learn disentangled representations and to control the facial attributes by manipulating the latent space. In low-level vision, the deep degradation representations can make it possible to decompose an image into content and degradation information, which can promote a number of new areas, such as degradation transferring and degradation editing. Further, more in-depth research on deep degradation representations will also greatly improve our understanding of the nature of images.

## References

- [1] Julius Adebayo, Justin Gilmer, Michael Muelly, Ian Goodfellow, Moritz Hardt, and Been Kim. Sanity checks for saliency maps. *arXiv preprint arXiv:1810.03292*, 2018.
- [2] Eirikur Agustsson and Radu Timofte. Ntire 2017 challenge on single image super-resolution: Dataset and study. In *The IEEE Conference on Computer Vision and Pattern Recognition (CVPR) Workshops*, July 2017.
- [3] Vijay Badrinarayanan, Alex Kendall, and Roberto Cipolla. Segnet: A deep convolutional encoder-decoder architecture for image segmentation. *IEEE transactions on pattern analysis and machine intelligence*, 39(12):2481–2495, 2017.
- [4] Bolun Cai, Xiangmin Xu, Kui Jia, Chunmei Qing, and Dacheng Tao. Dehazenet: An end-to-end system for single image haze removal. *IEEE Transactions on Image Processing*, 25(11):5187–5198, 2016.
- [5] Tadeusz Caliński and Jerzy Harabasz. A dendrite method for cluster analysis. *Communications in Statistics-theory and Methods*, 3(1):1–27, 1974.
- [6] Liang-Chieh Chen, George Papandreou, Florian Schroff, and Hartwig Adam. Rethinking atrous convolution for semantic image segmentation. *arXiv preprint arXiv:1706.05587*, 2017.
- [7] Tao Dai, Jianrui Cai, Yongbing Zhang, Shu-Tao Xia, and Lei Zhang. Second-order attention network for single image super-resolution. In *Proceedings of the IEEE/CVF Conference on Computer Vision and Pattern Recognition*, pages 11065–11074, 2019.
- [8] Pierre Demartines and Jeanny Hérault. Curvilinear component analysis: A self-organizing neural network for nonlinear mapping of data sets. *IEEE Transactions on neural networks*, 8(1):148–154, 1997.
- [9] Qili Deng, Ziling Huang, Chung-Chi Tsai, and Chia-Wen Lin. Hardgan: A haze-aware representation distillation gan for single image dehazing. In *European Conference on Computer Vision*, pages 722–738. Springer, 2020.
- [10] Yu Deng, Jiaolong Yang, Dong Chen, Fang Wen, and Xin Tong. Disentangled and controllable face image generation via 3d imitative-contrastive learning. In *Proceedings of the IEEE/CVF Conference on Computer Vision and Pattern Recognition (CVPR)*, June 2020.
- [11] Jeff Donahue, Yangqing Jia, Oriol Vinyals, Judy Hoffman, Ning Zhang, Eric Tzeng, and Trevor Darrell. Decaf: A deep convolutional activation feature for generic visual recognition. In *International conference on machine learning*, pages 647–655. PMLR, 2014.
- [12] Chao Dong, Chen Change Loy, Kaiming He, and Xiaoou Tang. Learning a deep convolutional network for image super-resolution. In *European conference on computer vision*, pages 184–199. Springer, 2014.
- [13] Chao Dong, Chen Change Loy, and Xiaoou Tang. Accelerating the super-resolution convolutional neural network. In *European conference on computer vision*, pages 391–407. Springer, 2016.
- [14] Yu Dong, Yihao Liu, He Zhang, Shifeng Chen, and Yu Qiao. Fd-gan: Generative adversarial networks with fusion-discriminator for single image dehazing. In *Proceedings of the AAAI Conference on Artificial Intelligence*, volume 34, pages 10729–10736, 2020.
- [15] Jinjin Gu, Hannan Lu, Wangmeng Zuo, and Chao Dong. Blind super-resolution with iterative kernel correction. In



Figure 9. Example images from different datasets. (a) DIV2k-clean. (b) DIV2k-noise20. (c) DIV2k-blur4. (d) DIV2k-mild. (e) Hollywood100. Different datasets contain different degradation types. (a), (b), (c) and (d) are aligned with image content, but contains degradations. The deep degradation representations (DDR) are discriminative to various degradations.

- Proceedings of the IEEE/CVF Conference on Computer Vision and Pattern Recognition*, pages 1604–1613, 2019.
- [16] Jiuxiang Gu, Zhenhua Wang, Jason Kuen, Lianyang Ma, Amir Shahroudy, Bing Shuai, Ting Liu, Xingxing Wang, Gang Wang, Jianfei Cai, et al. Recent advances in convolutional neural networks. *Pattern Recognition*, 77:354–377, 2018.
  - [17] Jingwen He, Yihao Liu, Yu Qiao, and Chao Dong. Conditional sequential modulation for efficient global image retouching. In *European Conference on Computer Vision*, pages 679–695. Springer, 2020.
  - [18] Kaiming He, Georgia Gkioxari, Piotr Dollár, and Ross Girshick. Mask r-cnn. In *Proceedings of the IEEE international conference on computer vision*, pages 2961–2969, 2017.
  - [19] Kaiming He, Xiangyu Zhang, Shaoqing Ren, and Jian Sun. Deep residual learning for image recognition. In *Proceedings of the IEEE conference on computer vision and pattern recognition*, pages 770–778, 2016.
  - [20] Geoffrey Hinton and Sam T Roweis. Stochastic neighbor embedding. In *NIPS*, volume 15, pages 833–840. Citeseer, 2002.
  - [21] Harold Hotelling. Analysis of a complex of statistical variables into principal components. *Journal of educational psychology*, 24(6):417, 1933.
  - [22] Jie Hu, Li Shen, and Gang Sun. Squeeze-and-excitation networks. In *Proceedings of the IEEE conference on computer vision and pattern recognition*, pages 7132–7141, 2018.
  - [23] Gao Huang, Zhuang Liu, Laurens Van Der Maaten, and Kilian Q Weinberger. Densely connected convolutional networks. In *Proceedings of the IEEE conference on computer vision and pattern recognition*, pages 4700–4708, 2017.
  - [24] W Ronny Huang, Zeyad Emam, Micah Goldblum, Liam Fowl, Justin K Terry, Furong Huang, and Tom Goldstein. Understanding generalization through visualizations. 2020.
  - [25] Sergey Ioffe and Christian Szegedy. Batch normalization: Accelerating deep network training by reducing internal covariate shift. In *International conference on machine learning*, pages 448–456. PMLR, 2015.
  - [26] Justin Johnson, Alexandre Alahi, and Li Fei-Fei. Perceptual losses for real-time style transfer and super-resolution. In *European conference on computer vision*, pages 694–711. Springer, 2016.
  - [27] Andrej Karpathy, Justin Johnson, and Li Fei-Fei. Visualizing and understanding recurrent networks. *arXiv preprint arXiv:1506.02078*, 2015.
  - [28] Tero Karras, Samuli Laine, and Timo Aila. A style-based generator architecture for generative adversarial networks. In *Proceedings of the IEEE/CVF Conference on Computer Vision and Pattern Recognition*, pages 4401–4410, 2019.
  - [29] Diederik P Kingma and Jimmy Ba. Adam: A method for stochastic optimization. *arXiv preprint arXiv:1412.6980*, 2014.
  - [30] Alex Krizhevsky, Ilya Sutskever, and Geoffrey E Hinton. Imagenet classification with deep convolutional neural networks. *Advances in neural information processing systems*, 25:1097–1105, 2012.
  - [31] Ivan Laptev, Marcin Marszalek, Cordelia Schmid, and Benjamin Rozenfeld. Learning realistic human actions from movies. In *2008 IEEE Computer Society Conference on Computer Vision and Pattern Recognition CVPR 2008*, 2008.
  - [32] Christian Ledig, Lucas Theis, Ferenc Huszár, Jose Caballero, Andrew Cunningham, Alejandro Acosta, Andrew Aitken, Alykhan Tejani, Johannes Totz, Zehan Wang, et al. Photo-realistic single image super-resolution using a generative adversarial network. In *Proceedings of the IEEE conference on computer vision and pattern recognition*, pages 4681–4690, 2017.
  - [33] Hsin-Ying Lee, Hung-Yu Tseng, Jia-Bin Huang, Maneesh Singh, and Ming-Hsuan Yang. Diverse image-to-image translation via disentangled representations. In *Proceedings of the European conference on computer vision (ECCV)*, pages 35–51, 2018.
  - [34] Seungmin Lee, Dongwan Kim, Namil Kim, and Seong-Gyun Jeong. Drop to adapt: Learning discriminative features for unsupervised domain adaptation. In *Proceedings of the IEEE/CVF International Conference on Computer Vision*, pages 91–100, 2019.
  - [35] Jiwei Li, Xinlei Chen, Eduard Hovy, and Dan Jurafsky. Visualizing and understanding neural models in nlp. *arXiv preprint arXiv:1506.01066*, 2015.
  - [36] Bee Lim, Sanghyun Son, Heewon Kim, Seungjun Nah, and Kyoung Mu Lee. Enhanced deep residual networks for single image super-resolution. In *Proceedings of the IEEE conference on computer vision and pattern recognition workshops*, pages 136–144, 2017.
  - [37] Jonathan Long, Evan Shelhamer, and Trevor Darrell. Fully convolutional networks for semantic segmentation. In *Proceedings of the IEEE conference on computer vision and pattern recognition*, pages 3431–3440, 2015.
  - [38] Liqian Ma, Qianru Sun, Stamatios Georgioulis, Luc Van Gool, Bernt Schiele, and Mario Fritz. Disentangled person image generation. In *Proceedings of the IEEE Conference on Computer Vision and Pattern Recognition*, pages 99–108, 2018.
  - [39] Aravindh Mahendran and Andrea Vedaldi. Visualizing deep convolutional neural networks using natural pre-images. *International Journal of Computer Vision*, 120(3):233–255, 2016.
  - [40] Volodymyr Mnih, Koray Kavukcuoglu, David Silver, Andrei A Rusu, Joel Veness, Marc G Bellemare, Alex Graves, Martin Riedmiller, Andreas K Fidjeland, Georg Ostrovski, et al. Human-level control through deep reinforcement learning. *nature*, 518(7540):529–533, 2015.
  - [41] Grégoire Montavon, Wojciech Samek, and Klaus-Robert Müller. Methods for interpreting and understanding deep neural networks. *Digital Signal Processing*, 73:1–15, 2018.
  - [42] Yotam Nitzan, Amit Bermano, Yangyan Li, and Daniel Cohen-Or. Face identity disentanglement via latent space mapping. *ACM Transactions on Graphics (TOG)*, 39(6):1–14, 2020.
  - [43] Aaron van den Oord, Yazhe Li, and Oriol Vinyals. Representation learning with contrastive predictive coding. *arXiv preprint arXiv:1807.03748*, 2018.

- [44] Yuhui Quan, Mingqin Chen, Tongyao Pang, and Hui Ji. Self2self with dropout: Learning self-supervised denoising from single image. In *Proceedings of the IEEE/CVF Conference on Computer Vision and Pattern Recognition*, pages 1890–1898, 2020.
- [45] Joseph Redmon, Santosh Divvala, Ross Girshick, and Ali Farhadi. You only look once: Unified, real-time object detection. In *Proceedings of the IEEE conference on computer vision and pattern recognition*, pages 779–788, 2016.
- [46] Shaoqing Ren, Kaiming He, Ross Girshick, and Jian Sun. Faster r-cnn: Towards real-time object detection with region proposal networks. *arXiv preprint arXiv:1506.01497*, 2015.
- [47] Sam T Roweis and Lawrence K Saul. Nonlinear dimensionality reduction by locally linear embedding. *science*, 290(5500):2323–2326, 2000.
- [48] Olga Russakovsky, Jia Deng, Hao Su, Jonathan Krause, Sanjeev Satheesh, Sean Ma, Zhiheng Huang, Andrej Karpathy, Aditya Khosla, Michael Bernstein, Alexander C. Berg, and Li Fei-Fei. ImageNet Large Scale Visual Recognition Challenge. *International Journal of Computer Vision (IJCV)*, 115(3):211–252, 2015.
- [49] Wojciech Samek, Thomas Wiegand, and Klaus-Robert Müller. Explainable artificial intelligence: Understanding, visualizing and interpreting deep learning models. *arXiv preprint arXiv:1708.08296*, 2017.
- [50] Ramprasaath R Selvaraju, Michael Cogswell, Abhishek Das, Ramakrishna Vedantam, Devi Parikh, and Dhruv Batra. Grad-cam: Visual explanations from deep networks via gradient-based localization. In *Proceedings of the IEEE international conference on computer vision*, pages 618–626, 2017.
- [51] Yujun Shen, Jinjin Gu, Xiaoou Tang, and Bolei Zhou. Interpreting the latent space of gans for semantic face editing. In *Proceedings of the IEEE/CVF Conference on Computer Vision and Pattern Recognition*, pages 9243–9252, 2020.
- [52] Yujun Shen, Ceyuan Yang, Xiaoou Tang, and Bolei Zhou. Interfacegan: Interpreting the disentangled face representation learned by gans. *IEEE Transactions on Pattern Analysis and Machine Intelligence*, 2020.
- [53] Yujun Shen and Bolei Zhou. Closed-form factorization of latent semantics in gans. *arXiv preprint arXiv:2007.06600*, 2020.
- [54] Wenzhe Shi, Jose Caballero, Ferenc Huszár, Johannes Totz, Andrew P Aitken, Rob Bishop, Daniel Rueckert, and Zehan Wang. Real-time single image and video super-resolution using an efficient sub-pixel convolutional neural network. In *Proceedings of the IEEE conference on computer vision and pattern recognition*, pages 1874–1883, 2016.
- [55] Karen Simonyan, Andrea Vedaldi, and Andrew Zisserman. Deep inside convolutional networks: Visualising image classification models and saliency maps. *arXiv preprint arXiv:1312.6034*, 2013.
- [56] K. Simonyan and A. Zisserman. Very deep convolutional networks for large-scale image recognition. In *International Conference on Learning Representations*, May 2015.
- [57] Christian Szegedy, Sergey Ioffe, Vincent Vanhoucke, and Alexander Alemi. Inception-v4, inception-resnet and the impact of residual connections on learning. In *Proceedings of the AAAI Conference on Artificial Intelligence*, volume 31, 2017.
- [58] Christian Szegedy, Wei Liu, Yangqing Jia, Pierre Sermanet, Scott Reed, Dragomir Anguelov, Dumitru Erhan, Vincent Vanhoucke, and Andrew Rabinovich. Going deeper with convolutions. In *Proceedings of the IEEE conference on computer vision and pattern recognition*, pages 1–9, 2015.
- [59] Joshua B Tenenbaum, Vin De Silva, and John C Langford. A global geometric framework for nonlinear dimensionality reduction. *science*, 290(5500):2319–2323, 2000.
- [60] Radu Timofte, Eirikur Agustsson, Luc Van Gool, Ming-Hsuan Yang, Lei Zhang, Bee Lim, et al. Ntire 2017 challenge on single image super-resolution: Methods and results. In *The IEEE Conference on Computer Vision and Pattern Recognition (CVPR) Workshops*, July 2017.
- [61] Radu Timofte, Shuhang Gu, Jiqing Wu, Luc Van Gool, Lei Zhang, Ming-Hsuan Yang, Muhammad Haris, et al. Ntire 2018 challenge on single image super-resolution: Methods and results. In *The IEEE Conference on Computer Vision and Pattern Recognition (CVPR) Workshops*, June 2018.
- [62] Laurens Van der Maaten and Geoffrey Hinton. Visualizing data using t-sne. *Journal of machine learning research*, 9(11), 2008.
- [63] Petar Veličković, Guillem Cucurull, Arantxa Casanova, Adriana Romero, Pietro Lio, and Yoshua Bengio. Graph attention networks. *arXiv preprint arXiv:1710.10903*, 2017.
- [64] Li Wang, Dong Li, Yousong Zhu, Lu Tian, and Yi Shan. Dual super-resolution learning for semantic segmentation. In *Proceedings of the IEEE/CVF Conference on Computer Vision and Pattern Recognition*, pages 3774–3783, 2020.
- [65] Xintao Wang, Ke Yu, Shixiang Wu, Jinjin Gu, Yihao Liu, Chao Dong, Yu Qiao, and Chen Change Loy. Esrgan: Enhanced super-resolution generative adversarial networks. In *European Conference on Computer Vision Workshops*, pages 63–79. Springer, 2018.
- [66] Yang Wang, Yang Cao, Zheng-Jun Zha, Jing Zhang, and Zhiwei Xiong. Deep degradation prior for low-quality image classification. In *Proceedings of the IEEE/CVF Conference on Computer Vision and Pattern Recognition*, pages 11049–11058, 2020.
- [67] Yandong Wen, Kaipeng Zhang, Zhifeng Li, and Yu Qiao. A discriminative feature learning approach for deep face recognition. In *European conference on computer vision*, pages 499–515. Springer, 2016.
- [68] Tom Zahavy, Nir Ben-Zrihem, and Shie Mannor. Graying the black box: Understanding dqns. In *International Conference on Machine Learning*, pages 1899–1908. PMLR, 2016.
- [69] Matthew D Zeiler and Rob Fergus. Visualizing and understanding convolutional networks. In *European conference on computer vision*, pages 818–833. Springer, 2014.
- [70] Matthew D Zeiler, Dilip Krishnan, Graham W Taylor, and Rob Fergus. Deconvolutional networks. In *2010 IEEE Computer Society Conference on computer vision and pattern recognition*, pages 2528–2535. IEEE, 2010.
- [71] He Zhang and Vishal M Patel. Densely connected pyramid dehazing network. In *Proceedings of the IEEE conference on computer vision and pattern recognition*, pages 3194–3203, 2018.



- [72] Kai Zhang, Wangmeng Zuo, Yunjin Chen, Deyu Meng, and Lei Zhang. Beyond a gaussian denoiser: Residual learning of deep cnn for image denoising. *IEEE transactions on image processing*, 26(7):3142–3155, 2017.
- [73] Kai Zhang, Wangmeng Zuo, and Lei Zhang. Ffdnet: Toward a fast and flexible solution for cnn-based image denoising. *IEEE Transactions on Image Processing*, 27(9):4608–4622, 2018.
- [74] Wenlong Zhang, Yihao Liu, Chao Dong, and Yu Qiao. Ranksrgan: Generative adversarial networks with ranker for image super-resolution. In *Proceedings of the IEEE/CVF International Conference on Computer Vision*, pages 3096–3105, 2019.
- [75] Yulun Zhang, Kunpeng Li, Kai Li, Lichen Wang, Bineng Zhong, and Yun Fu. Image super-resolution using very deep residual channel attention networks. In *Proceedings of the European conference on computer vision (ECCV)*, pages 286–301, 2018.
- [76] Yulun Zhang, Yapeng Tian, Yu Kong, Bineng Zhong, and Yun Fu. Residual dense network for image super-resolution. In *Proceedings of the IEEE conference on computer vision and pattern recognition*, pages 2472–2481, 2018.
- [77] Yu Zhang, Peter Tiño, Aleš Leonardis, and Ke Tang. A survey on neural network interpretability. *arXiv preprint arXiv:2012.14261*, 2020.
- [78] Bolei Zhou, Aditya Khosla, Agata Lapedriza, Aude Oliva, and Antonio Torralba. Learning deep features for discriminative localization. In *Proceedings of the IEEE conference on computer vision and pattern recognition*, pages 2921–2929, 2016.
- [79] Bo Zhu, Jeremiah Z Liu, Stephen F Cauley, Bruce R Rosen, and Matthew S Rosen. Image reconstruction by domain-transform manifold learning. *Nature*, 555(7697):487–492, 2018.